Supporting Information

One-step synthesis of $MnS/MoS_2/C$ through calcination and sulfurization of a bi-metal-organic framework for high-performance supercapacitor and its photocurrent investigation

Zhi Shuo Yan,[a] Ji Ying Long,[a] Qing Feng Zhou,[a] Yun Gong,*[a] and Jian Hua Lin*[a, b]

[a] *Department of Applied Chemistry, College of Chemistry and Chemical Engineering,Chongqing University, Chongqing 401331, P. R. China.*

E-mail: gongyun7211@cqu.edu.cn; Tel: +86-023-65678932.

[b] *State Key Laboratory of Rare Earth Materials Chemistry and Applications, College of Chemistry and Molecular Engineering, Peking University, Beijing 100871, P. R. China.*

E-mail: jhlin@pku.edu.cn; Tel:+86-010-62753541.

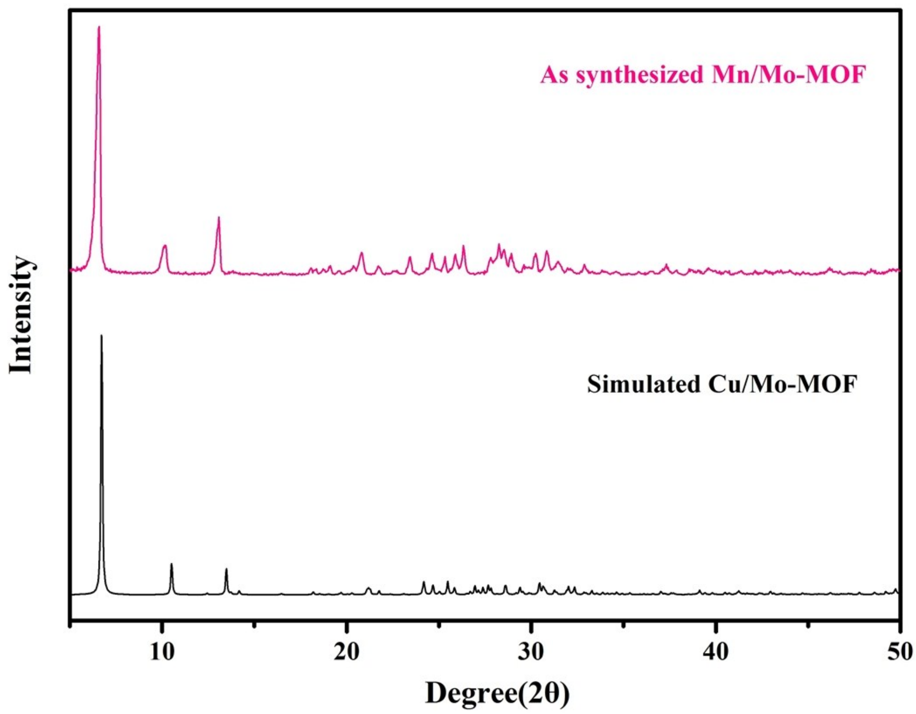

Fig. S1 The PXRD pattern of the as-synthesized Mn/Mo-MOF.

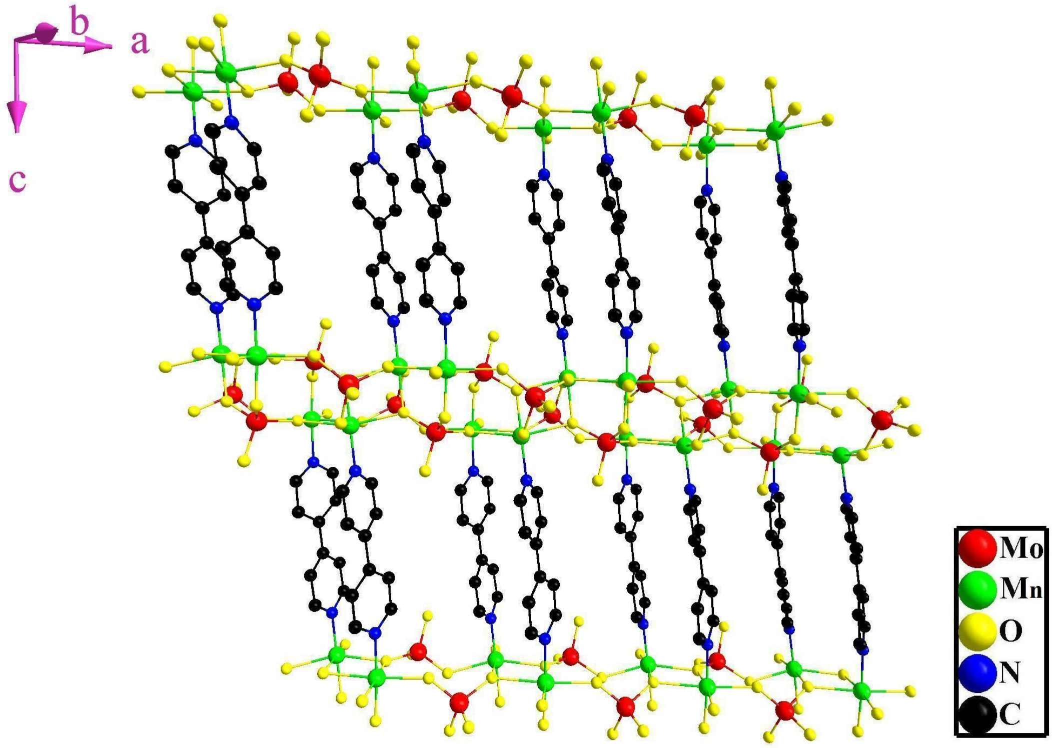

Fig. S2 The 3D architecture of the Mn/Mo-MOF highlighting the coordination environment of the Mn and Mo atoms (H atoms omitted for clarity).

(a)

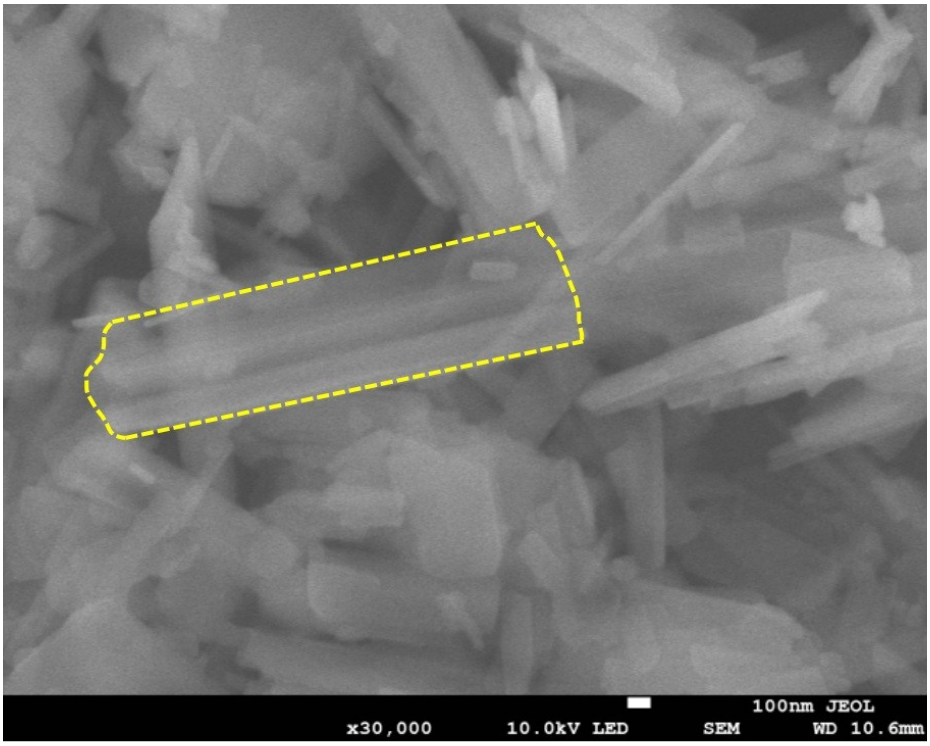

(**b**)

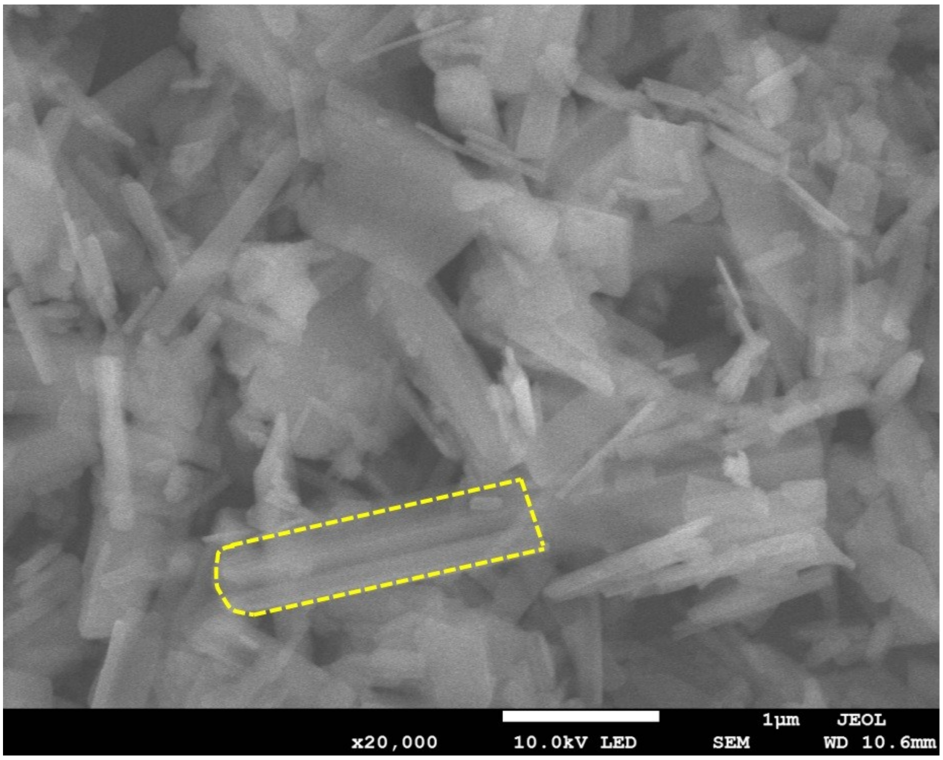

Fig. S3 The SEM images of the Mn/Mo-MOF at different magnifications (**a**, **b**).

(**a**)

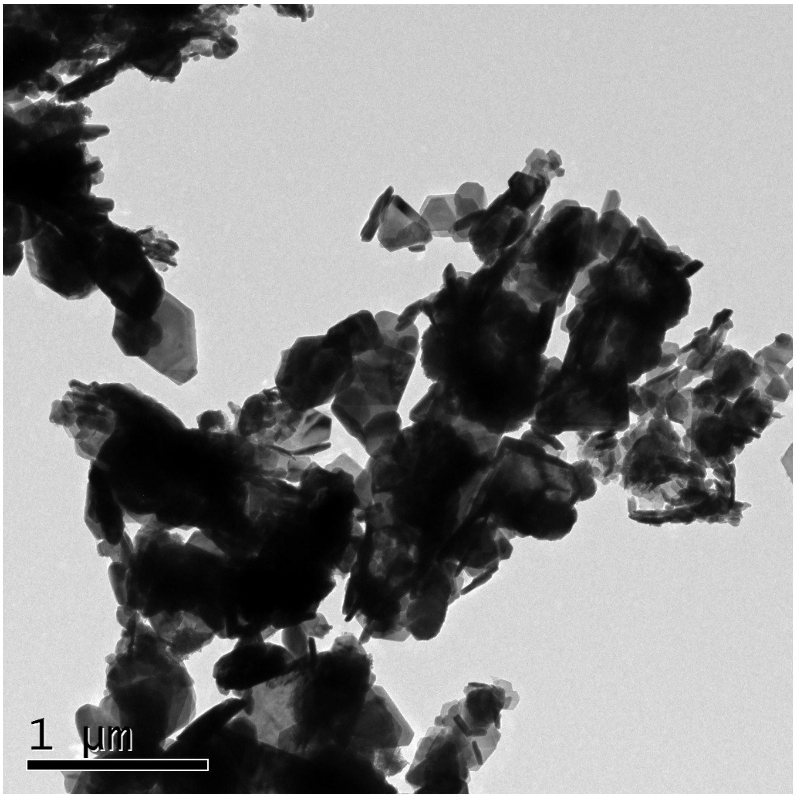

(**b**)

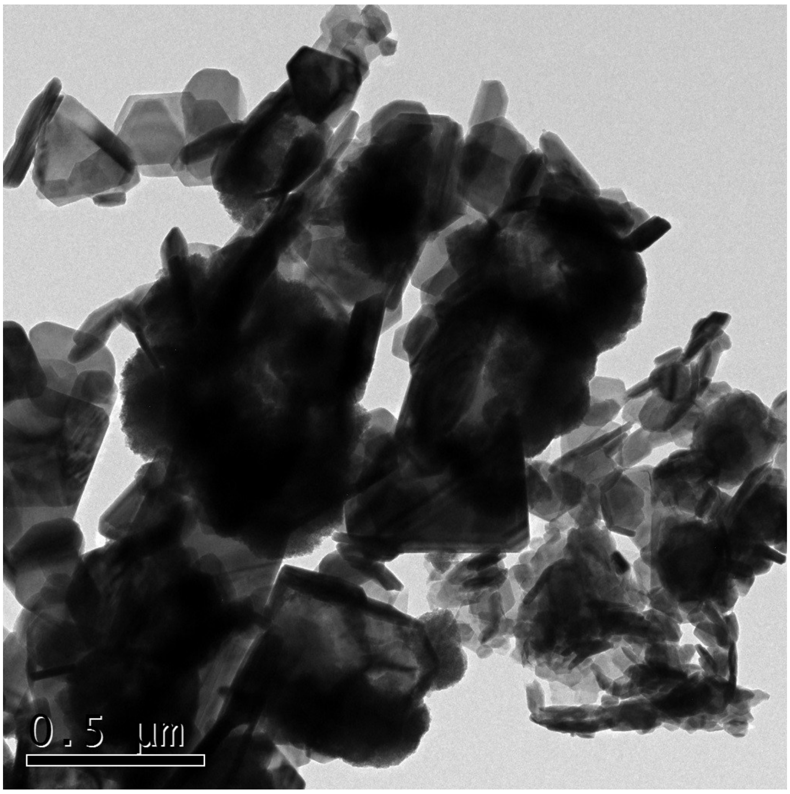

Fig. S4 The TEM images of the $MnS/MoS_2/C$ hybrid at different magnifications (**a**, **b**).

(**a**)

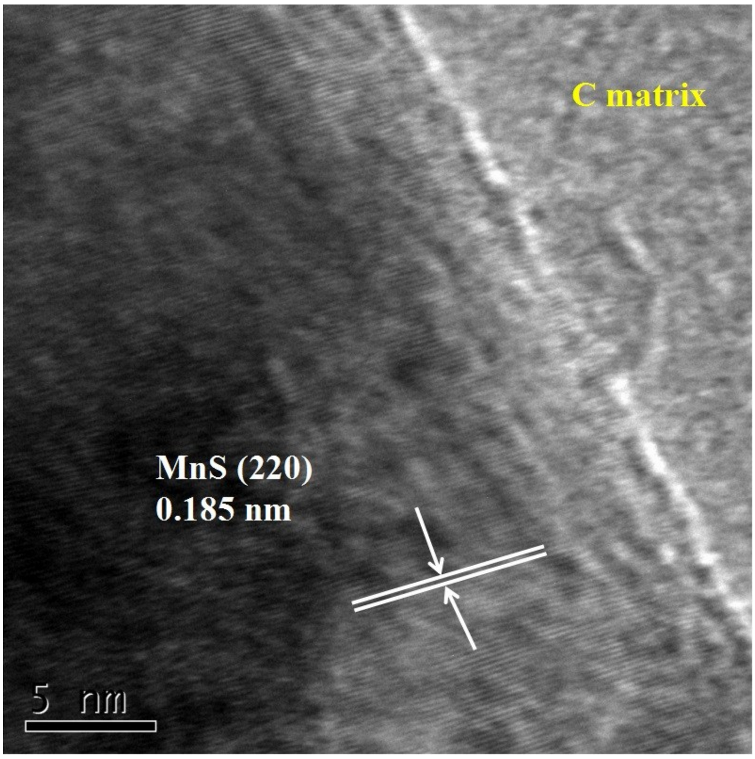

(**b**)

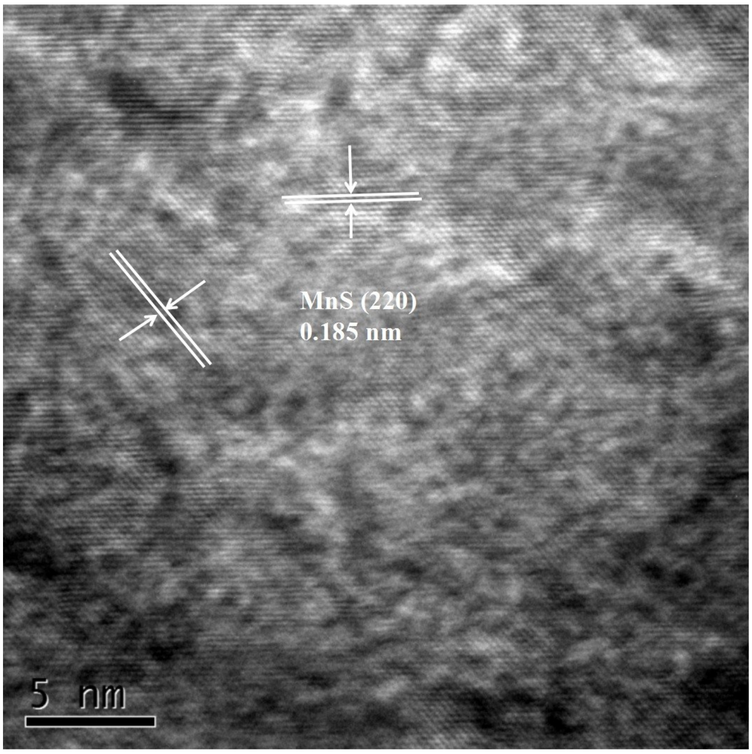

(**c**)

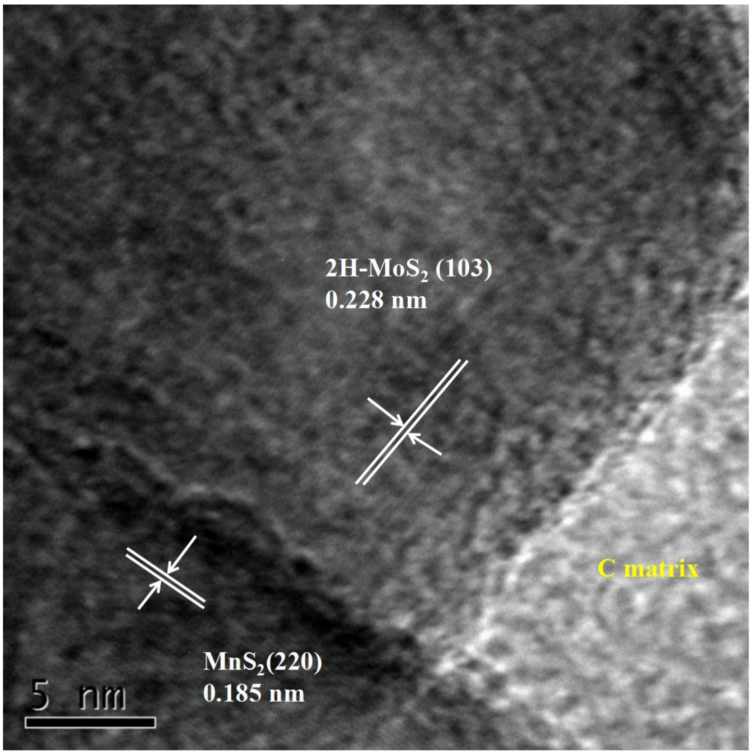

Fig. S5 The HR-TEM images of the MnS/MoS_2/C hybrid (**a-c**).

Table S1 The atom % in the MnS/MoS_2/C hybrid before and after the electrochemical measurement.

Atom %	The original sample	After 10000 GCD cycles
Mn	8.3 [a]/6.3 [b]/7.3 [c]	21.3 [d]/17.0 [e]
Mo	9.6 [a]/8.0 [b]/9.1 [c]	0 [d]/0 [e]
S	27.5 [a]/22.4 [b]/24.5 [c]	1.9 [d]/1.3 [e]
C	34.9 [a]/38.9 [b]/36.7 [c]	19.8 [d]/20.5 [e]
O	19.6 [a]/23.0 [b]/22.5 [c]	53.4 [d]/59.0 [e]
N	0 [a]/1.3 [b]/0 [c]	3.7 [d]/2.2 [e]

[a-c)] The percentages of the atoms are calculated based on the EDS data in **Fig. 3e-g**.

[c, d)] The percentages of the atoms are calculated based on the EDS data in **Fig. S18a-b**.

(a) **(b)**

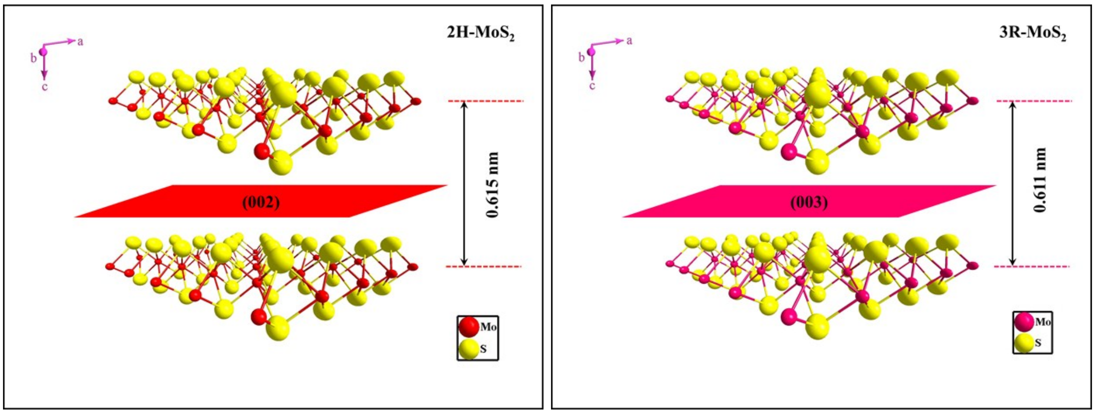

Fig. S6 The 2H-(002) (**a**) and 3R-(003) crystalline planes of the MoS_2 (**b**).

(a) **(b)**

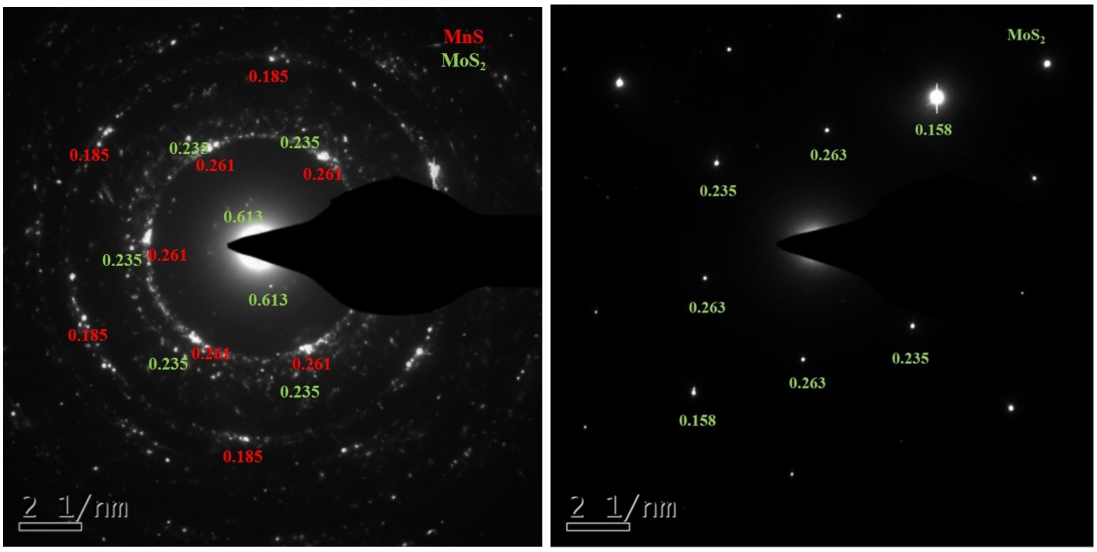

Fig. S7 The SAED patterns of the $MnS/MoS_2/C$ hybrid (**a, b**).

(a)

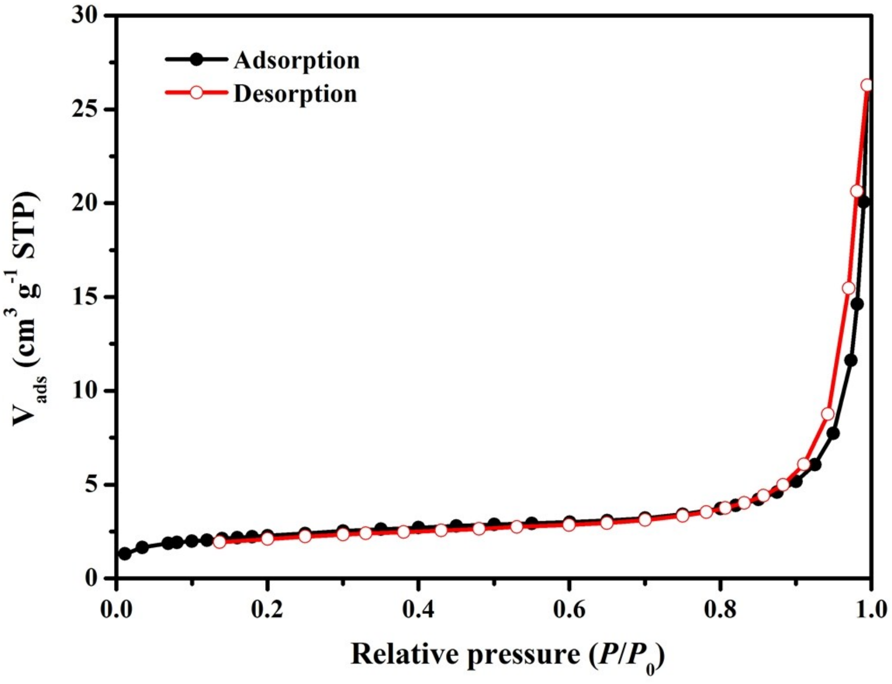

(**b**)

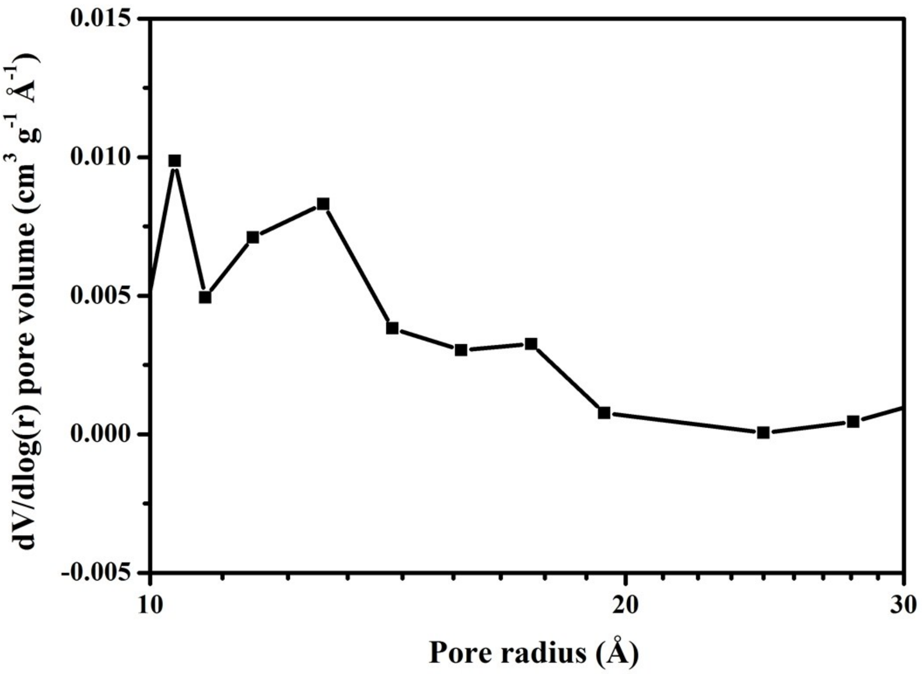

Fig. S8 N_2 adsorption and desorption isotherm curves (**a**) and BJH desorption pore size distribution of the $MnS/MoS_2/C$ hybrid material (**b**).

(**a**)

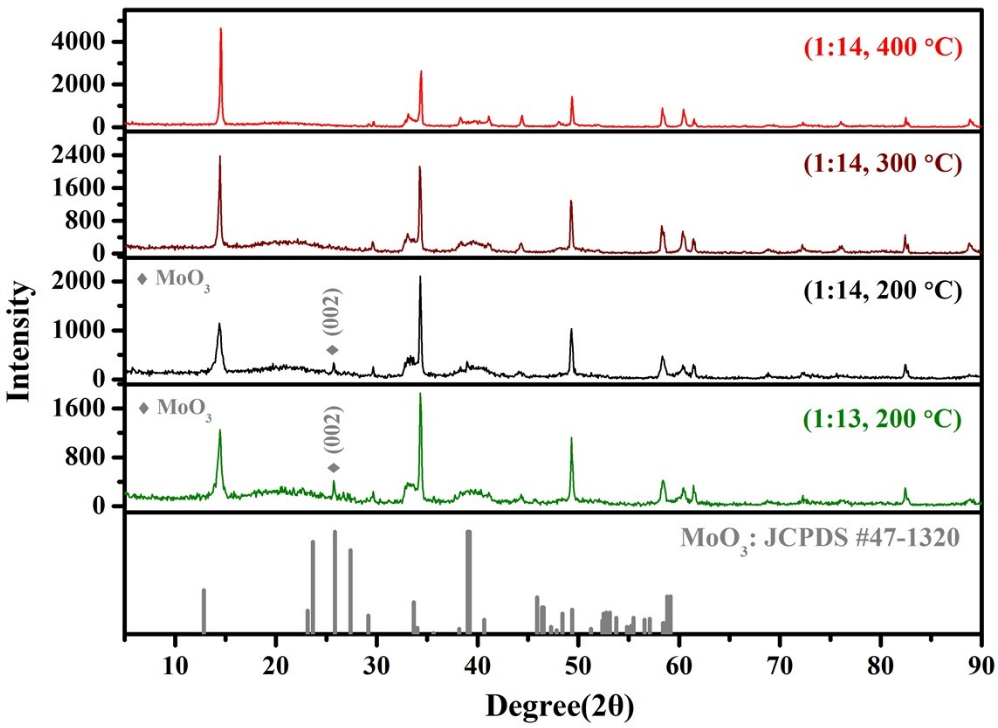

(**b**)

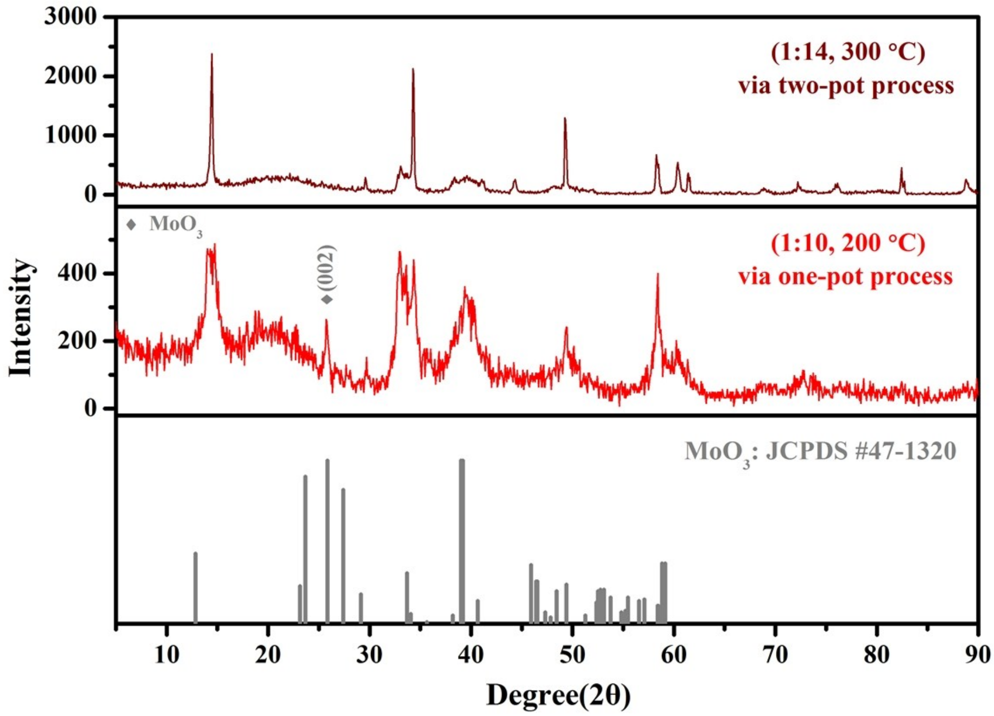

Fig. S9 The PXRD patterns of the calcined samples under different conditions: in a two-pot process with different temperatures and molar ratios of MOF/S (**a**); in two-pot (300 ℃, MOF/S=1: 14) and one-pot process (200 ℃, MOF/S=1: 10) (**b**).

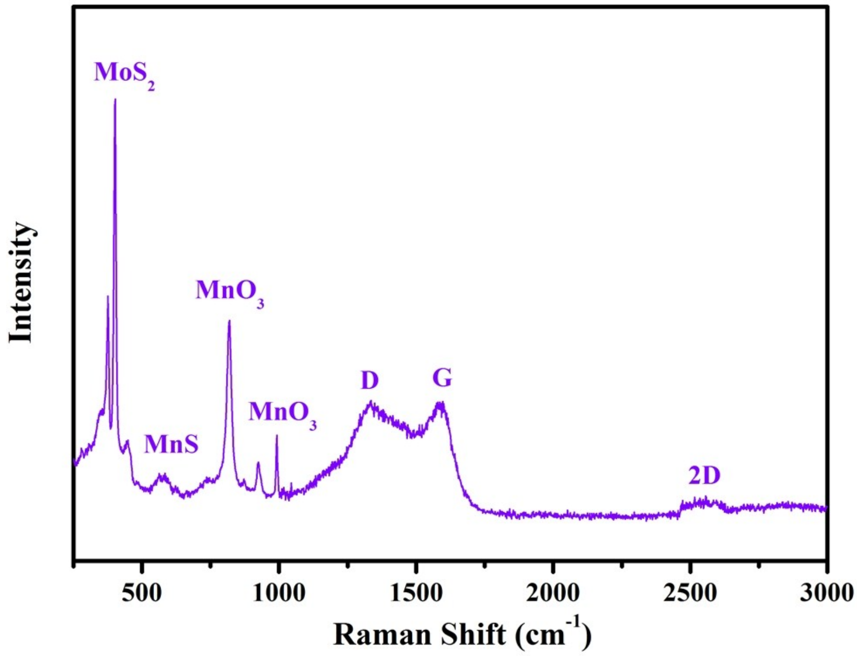

Fig. S10 Raman spectrum of the calcined sample via one-pot method (200 ℃, MOF/S=1: 10).

(**a**)

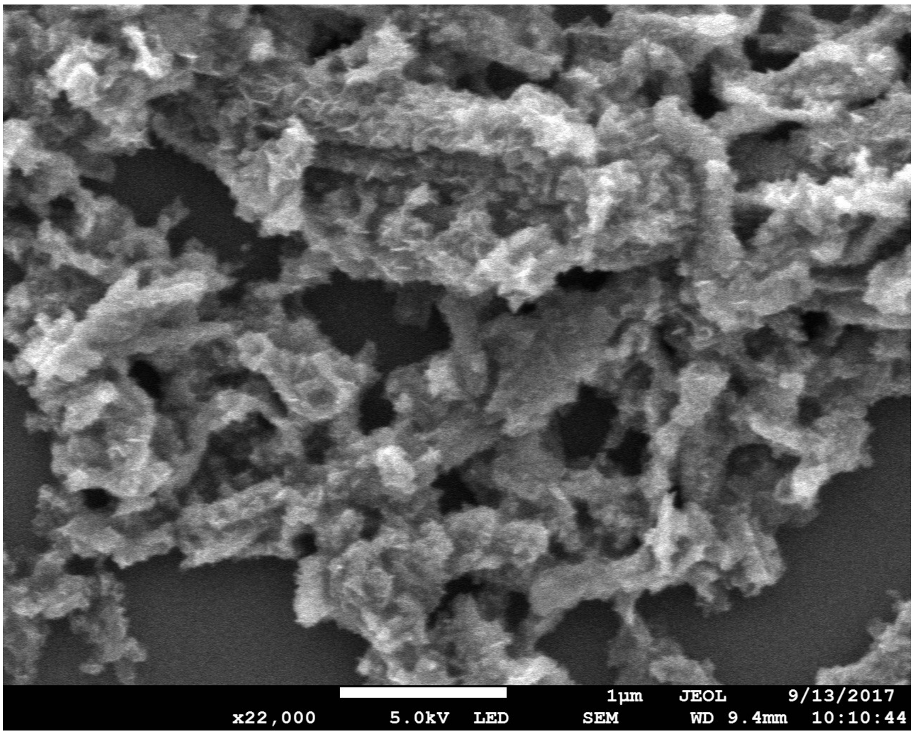
1µm JEOL 9/13/2017
x22,000 5.0kV LED SEM WD 9.4mm 10:10:44

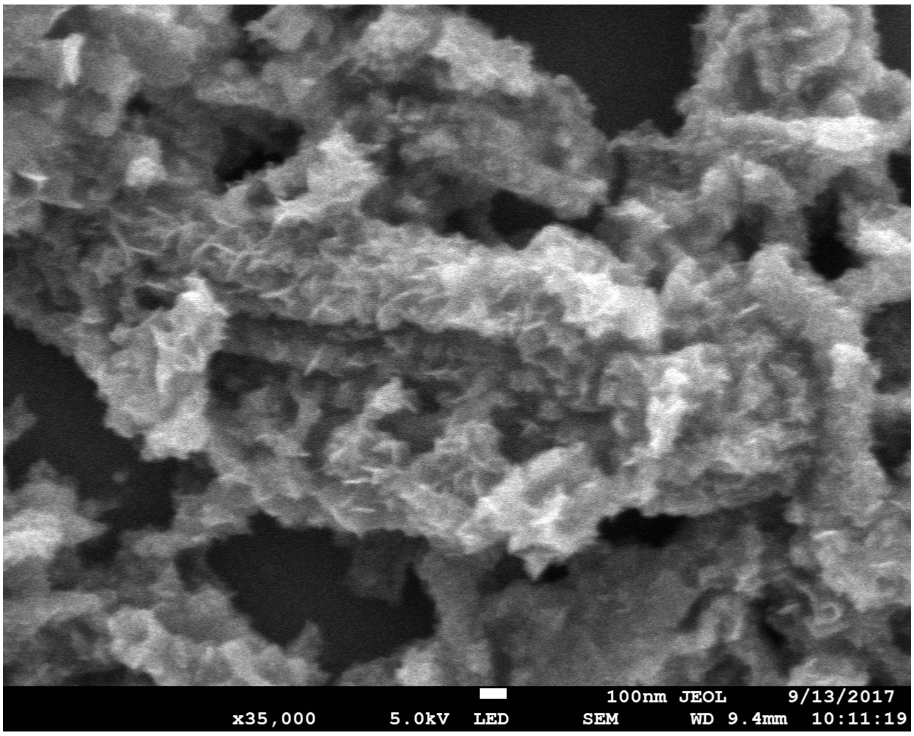
100nm JEOL 9/13/2017
x35,000 5.0kV LED SEM WD 9.4mm 10:11:19

(b)

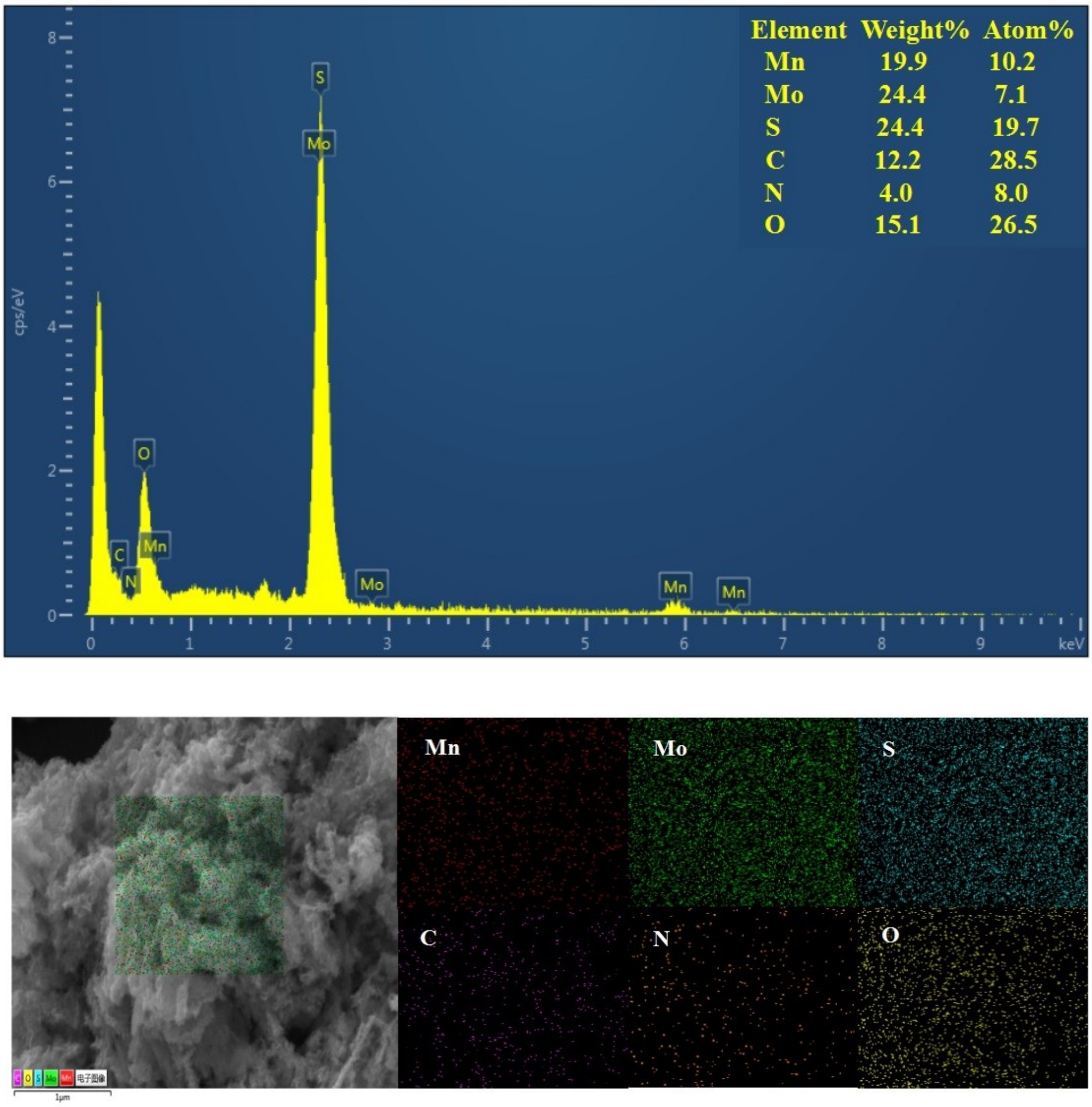

Element Weight% Atom%
Mn 19.9 10.2
Mo 24.4 7.1
S 24.4 19.7
C 12.2 28.5
N 4.0 8.0
O 15.1 26.5
cps/eV
keV
S
Mo
O
C
N
Mn
Mo
Mn
Mn
Mn
Mo
S
C
N
O
1μm

(c)

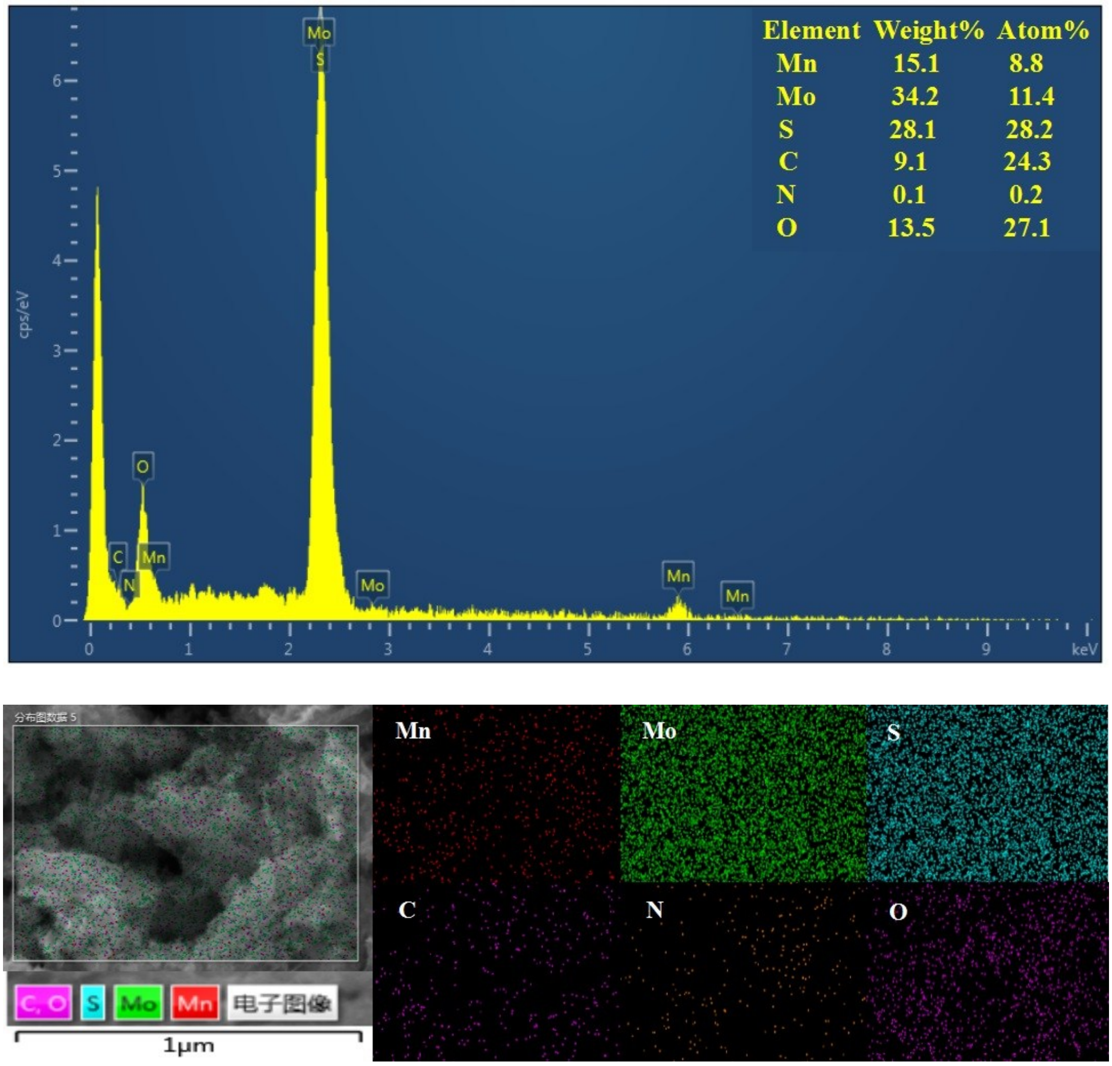

Fig. S11 SEM images (**a**); EDS and elemental mappings (**b**, **c**) of the calcined sample via one-pot method (200 ℃， MOF/S=1: 10).

(**a**)

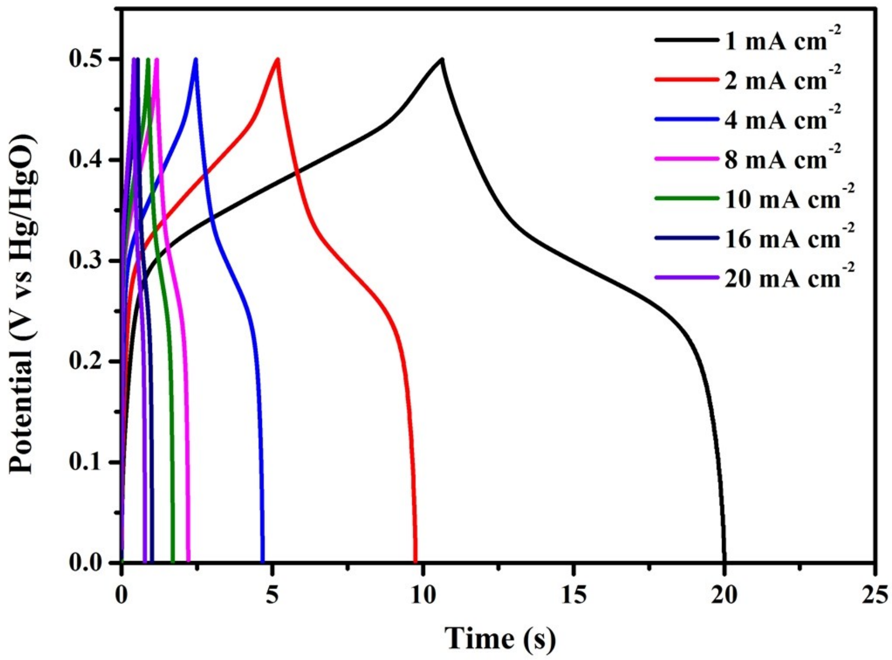

(**b**)

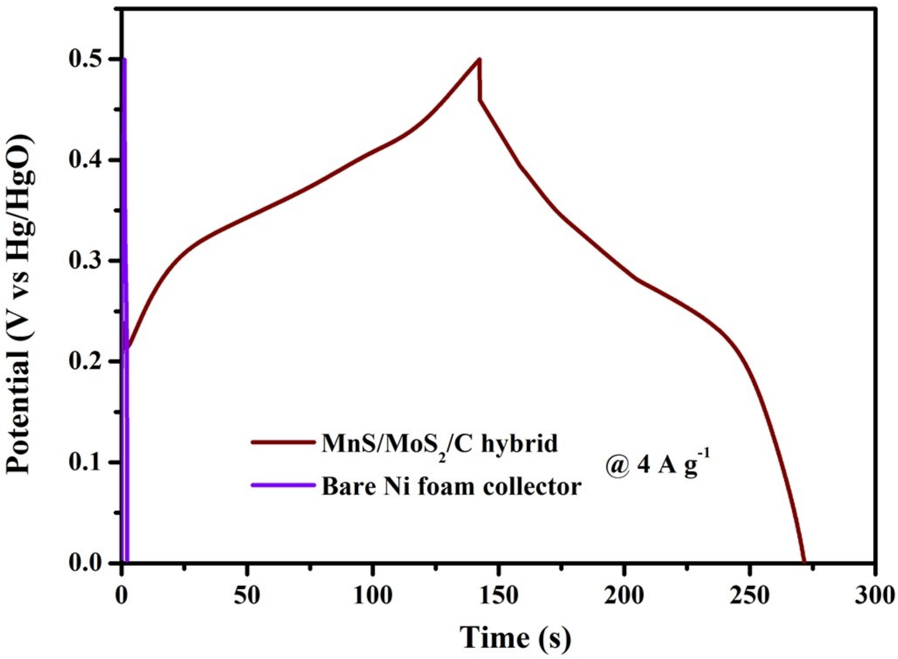

Fig. S12 Three-electrode electrochemical measurements for bare Ni foam collector in 2 M KOH aqueous solution: GCD curves (**a**) and comparison with $MnS/MoS_2/C$

hybrid at discharge current density of 4 A g^{-1} (**b**).

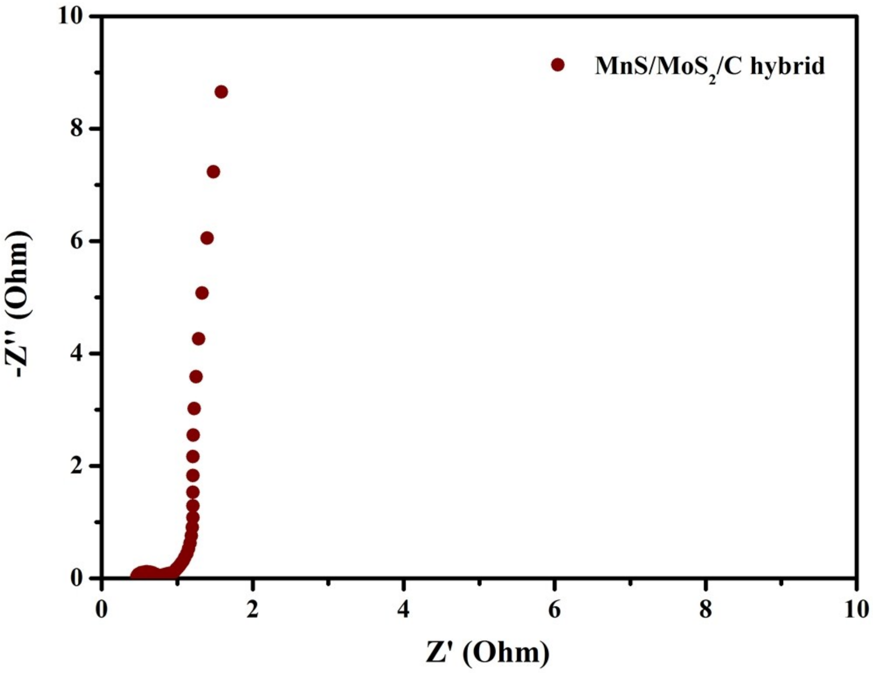

Fig. S13 Nyquist plots of the MnS/MoS$_2$/C hybrid material in 2 M KOH at a potential of 0 V vs Hg/HgO.

(**a**)

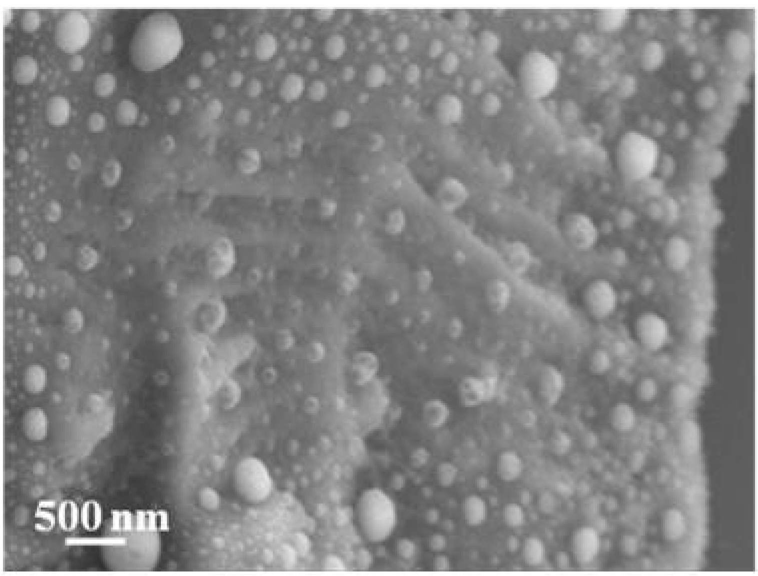

(**b**)

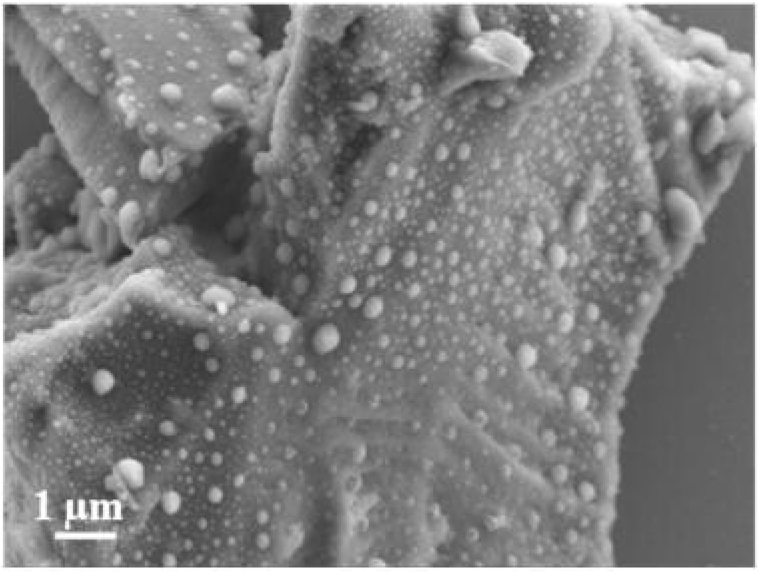

Fig. S14 SEM images of the commercial activated carbon (AC) (**a**, **b**).

(**a**)

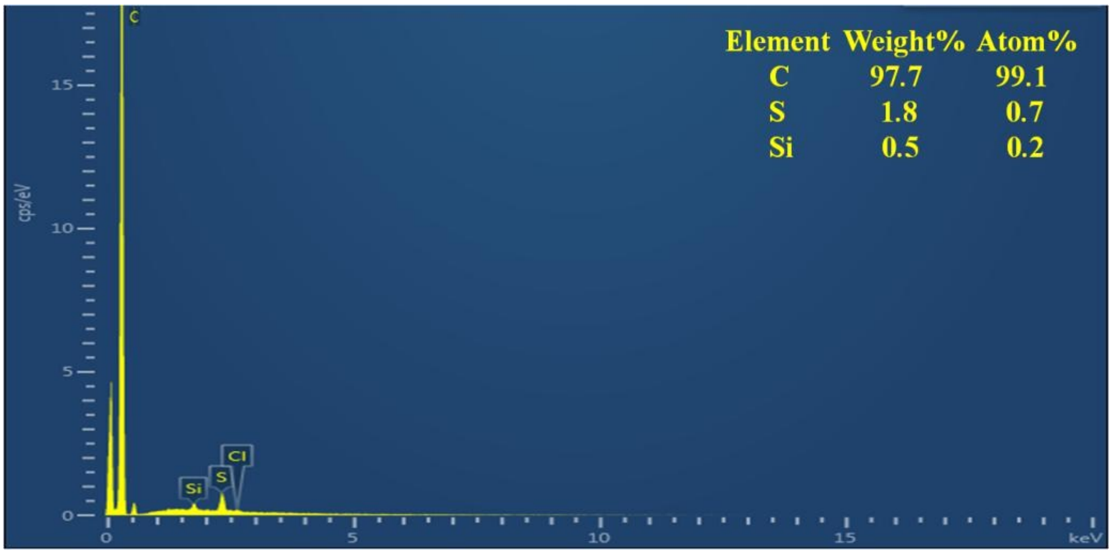

(**b**)

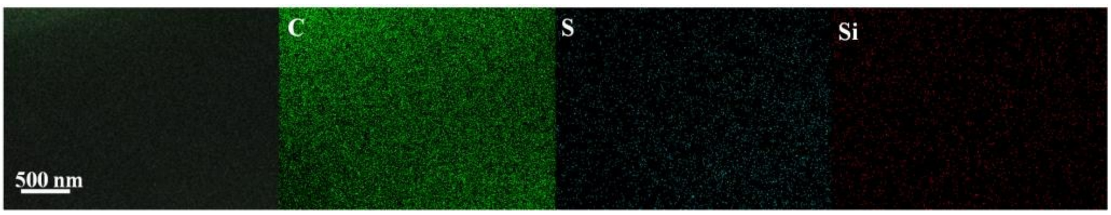

Fig. S15 EDS (**a**) and elemental mappings of the AC (**b**).

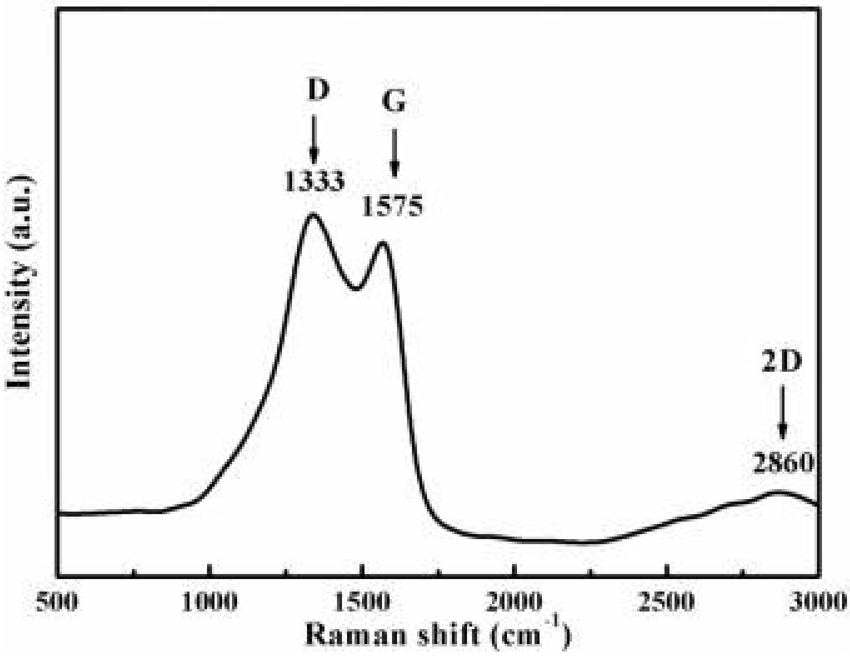

Fig. S16 Raman spectrum of the AC.

(**a**)

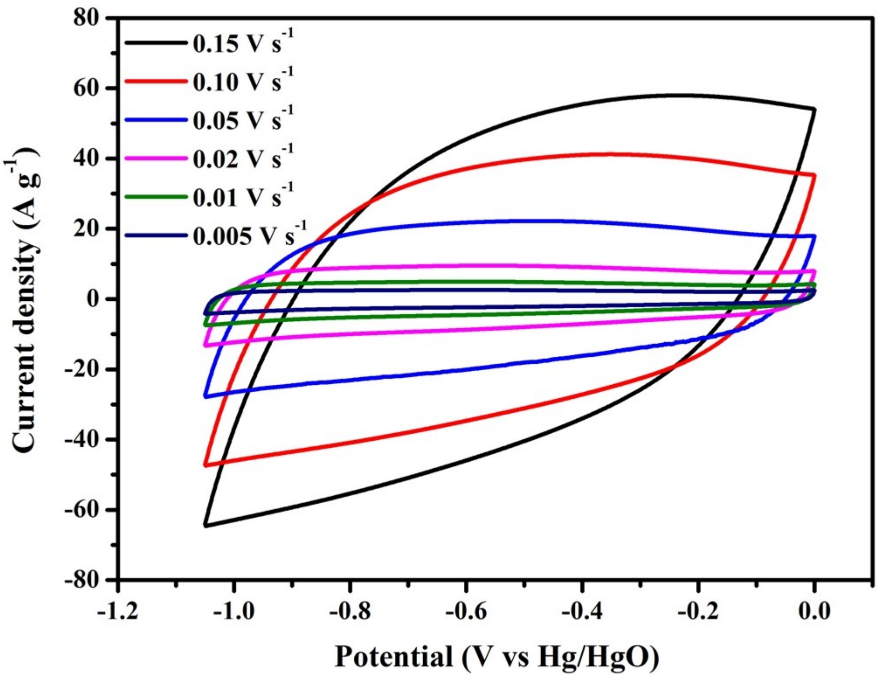

(**b**)

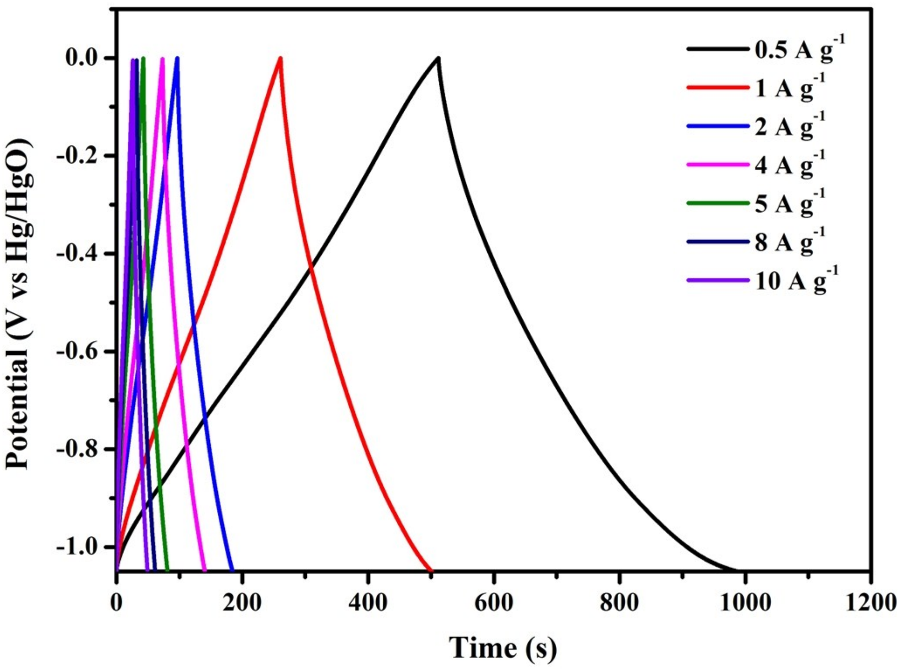

0.5 A g-1
1 A g-1
2 A g-1
4 A g-1
5 A g-1
8 A g-1
10 A g-1
Potential (V vs Hg/HgO)
0.0
-0.2
-0.4
-0.6
-0.8
-1.0
0
200
400
600
800
1000
1200
Time (s)

(**c**)

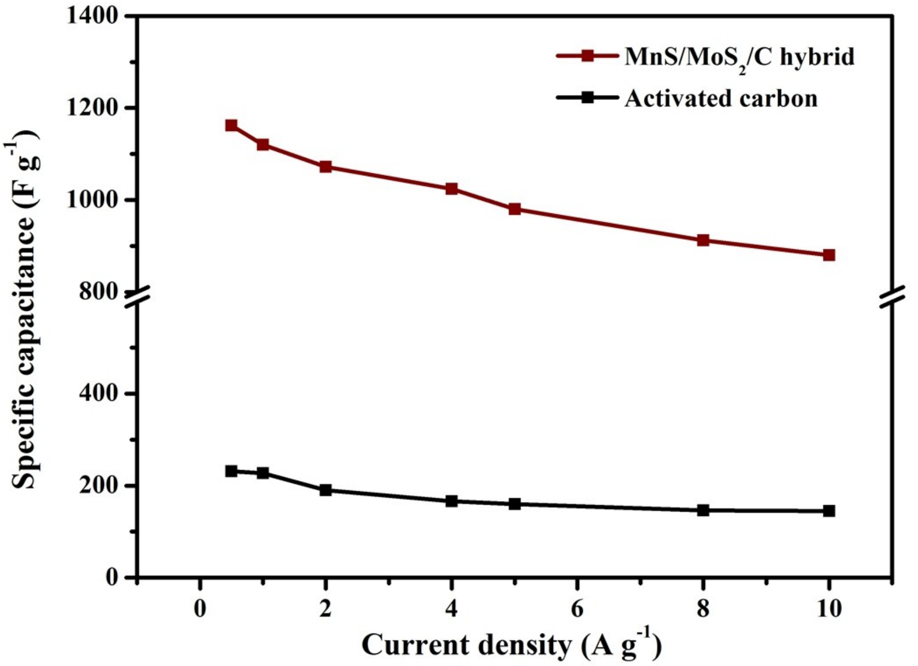

MnS/MoS2/C hybrid
Activated carbon
Specific capacitance (F g-1)
1400
1200
1000
800
400
200
0
0
2
4
6
8
10
Current density (A g-1)

(**d**)

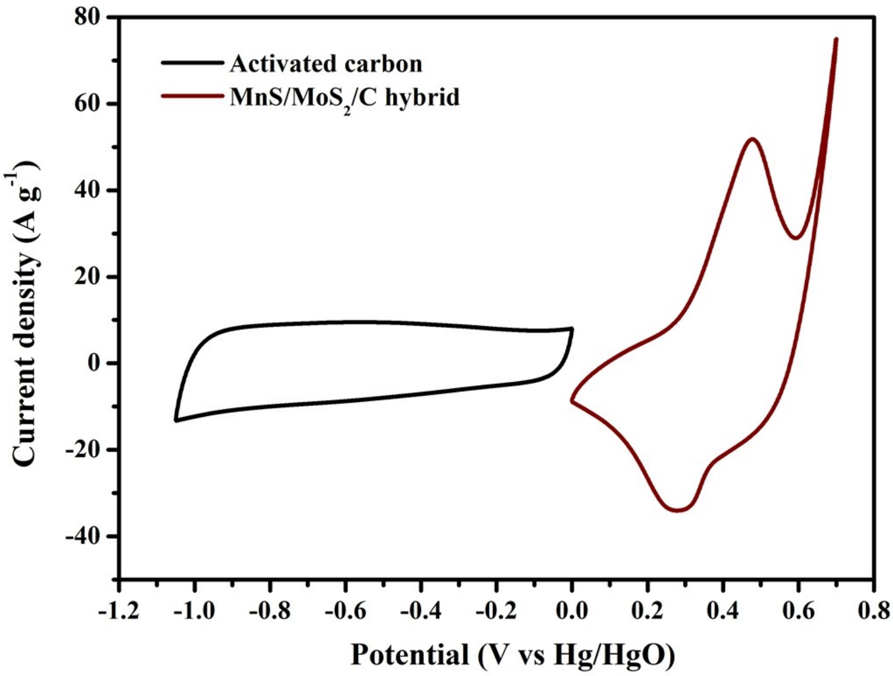

Fig. S17 Three-electrode electrochemical measurements in 2M KOH aqueous solution: CV curves of the AC at various scan rates (**a**) and GCD curves of the AC at various current densities (**b**); specific capacitances at various current densities (**c**) and CV curves at 0.02 V s^{-1} of the $MnS/MoS_2/C$ hybrid and the AC (**d**).

(**a**)

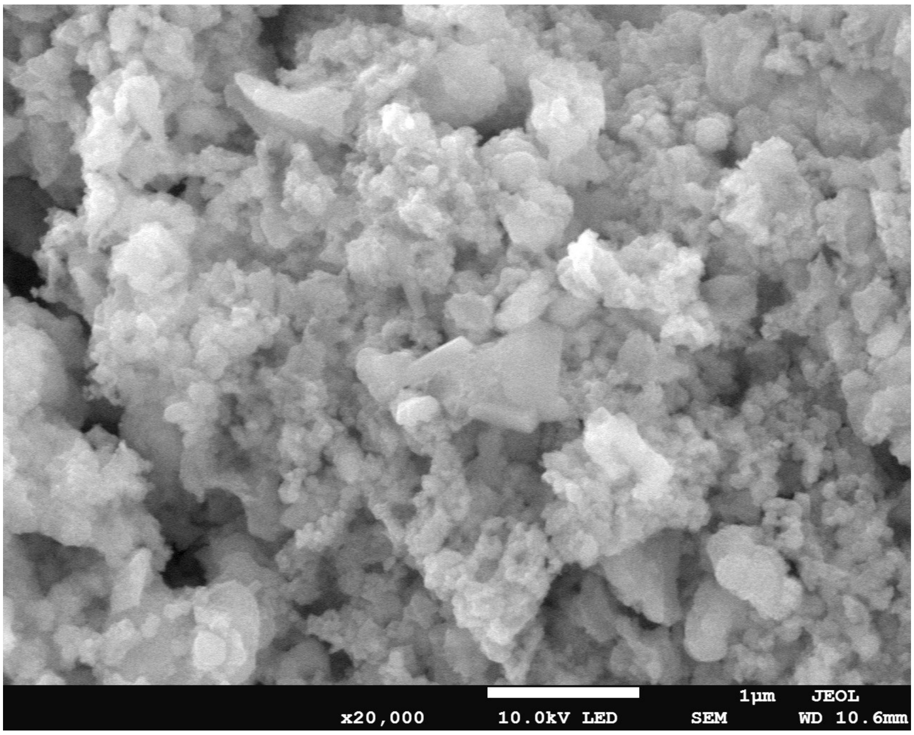

(**b**)

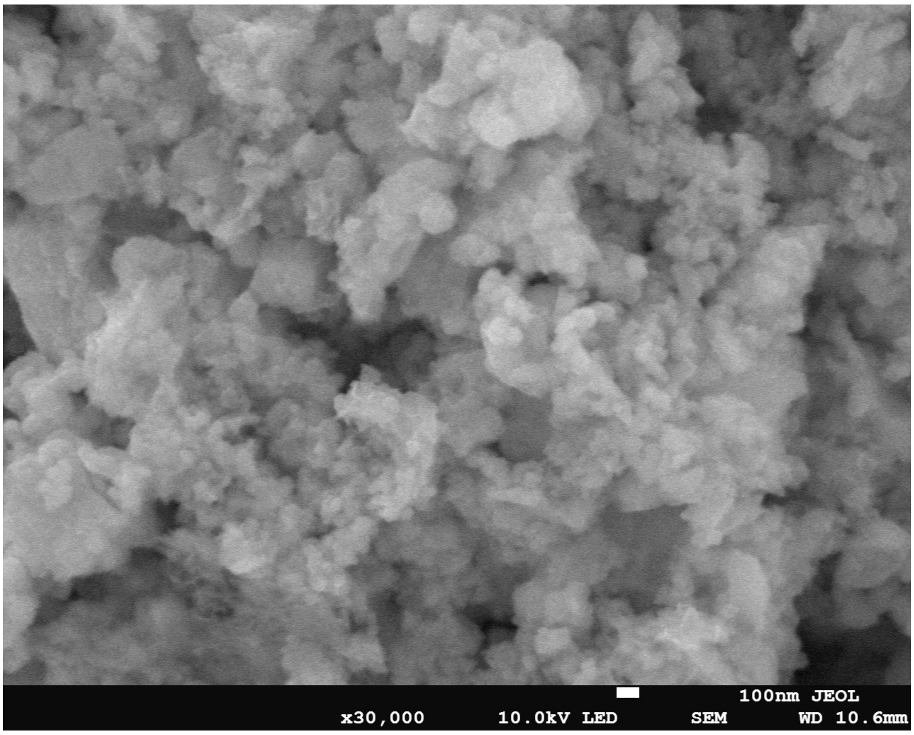

Fig. S18 SEM images of the MnS/MoS$_2$/C hybrid after 10000 GCD cycles (**a**, **b**).

(**a**)

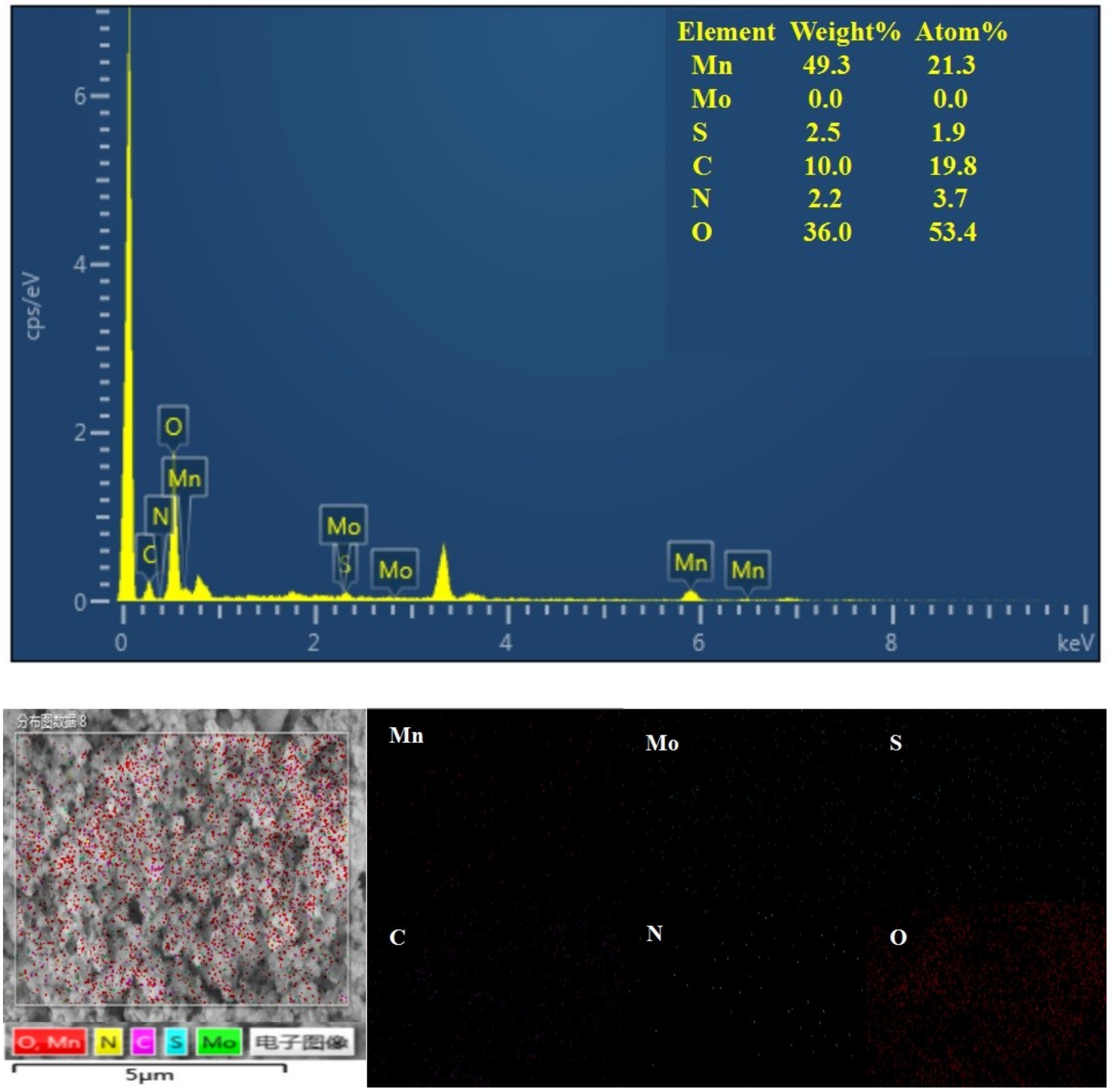
Element Weight% Atom%
Mn 49.3 21.3
Mo 0.0 0.0
S 2.5 1.9
C 10.0 19.8
N 2.2 3.7
O 36.0 53.4
cps/eV
keV
分布图数据 8
O, Mn
N
C
S
Mo
电子图像
5μm
Mn
Mo
S
C
N
O

(b)

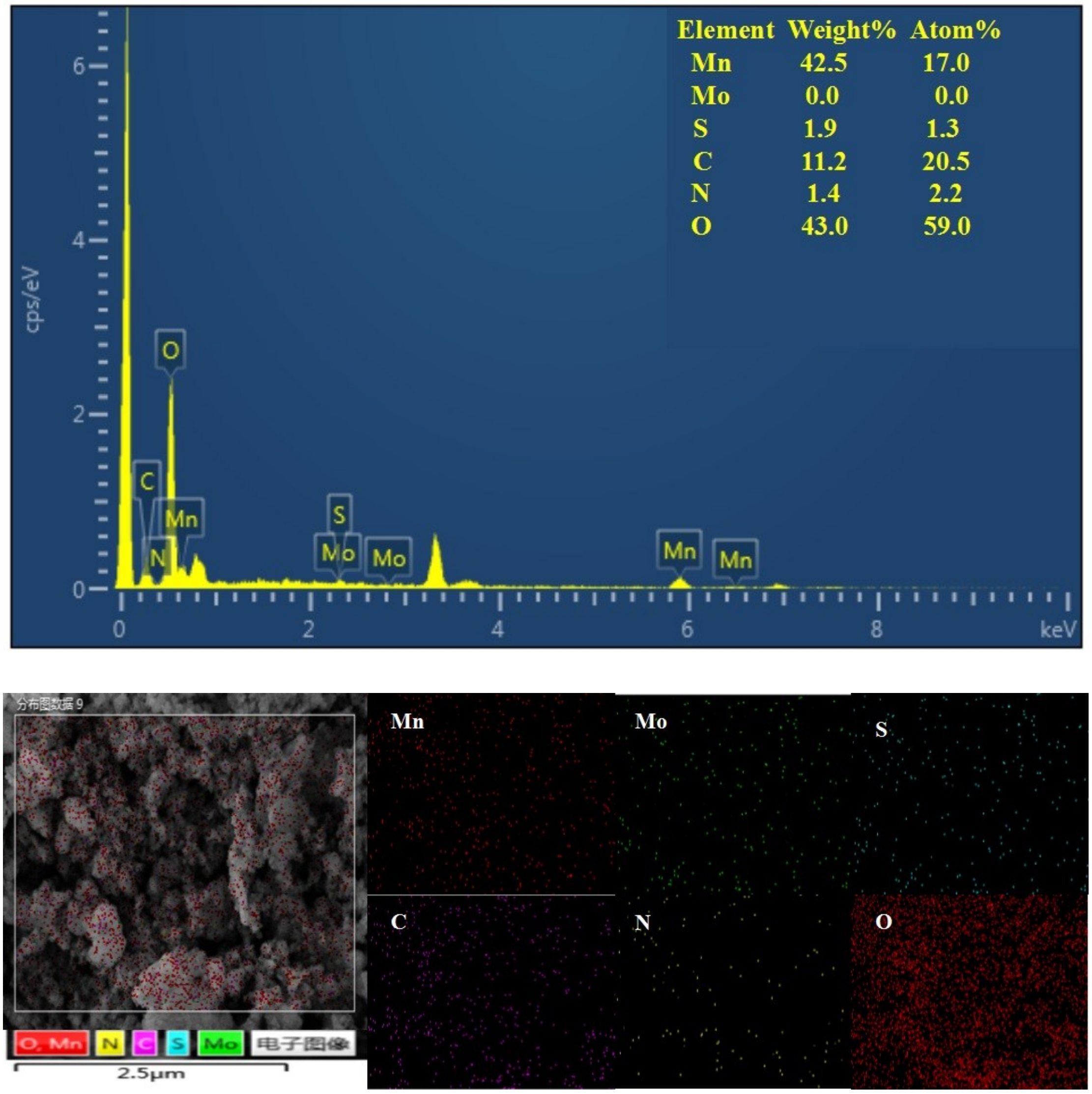

Fig. S19 EDS (top) and the corresponding elemental mappings (bottom) of the $MnS/MoS_2/C$ hybrid after 10000 charge-discharge cycles at two randomly selected regions (**a**, **b**).

(**a**)

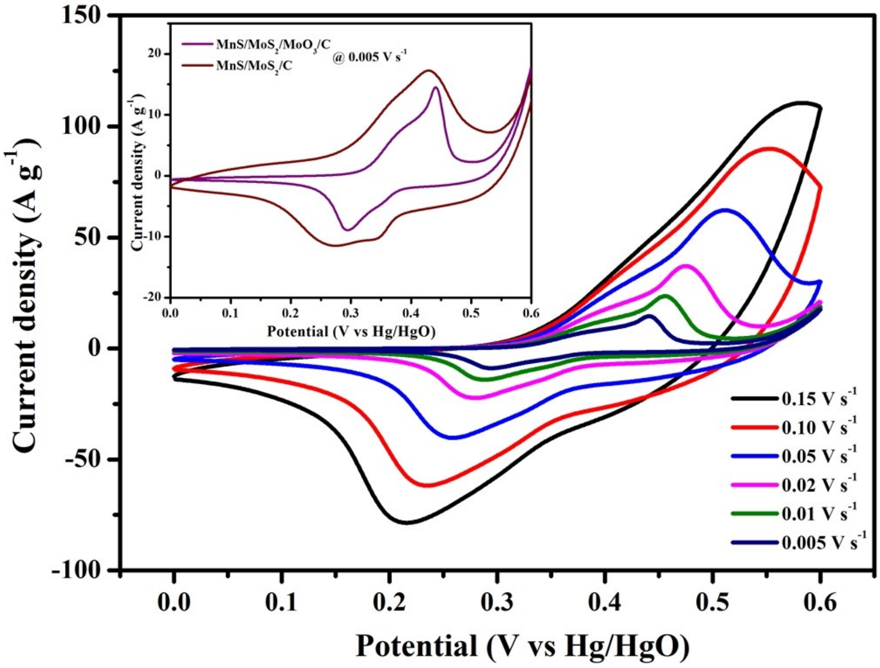
Current density (A g^{-1})
Potential (V vs Hg/HgO)
0.15 V s^{-1}
0.10 V s^{-1}
0.05 V s^{-1}
0.02 V s^{-1}
0.01 V s^{-1}
0.005 V s^{-1}
MnS/MoS$_2$/MoO$_3$/C
MnS/MoS$_2$/C
@ 0.005 V s^{-1}

(**b**)

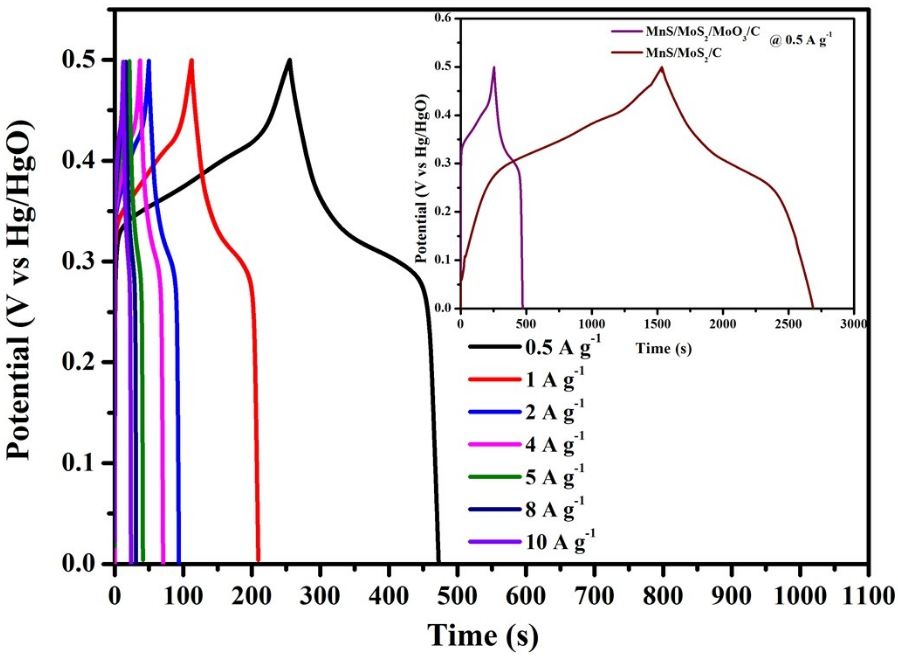
Potential (V vs Hg/HgO)
Time (s)
0.5 A g^{-1}
1 A g^{-1}
2 A g^{-1}
4 A g^{-1}
5 A g^{-1}
8 A g^{-1}
10 A g^{-1}
MnS/MoS$_2$/MoO$_3$/C
MnS/MoS$_2$/C
@ 0.5 A g^{-1}

(**c**)

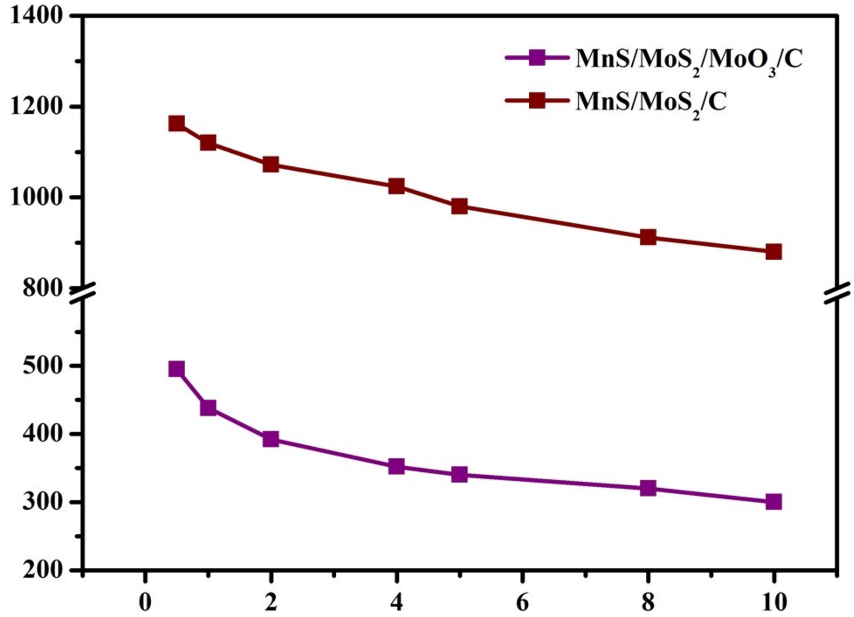

Fig. S20 Three-electrode electrochemical measurements of the $MnS/MoS_2/MoO_3/C$ in 2 M KOH aqueous solution for comparison with $MnS/MoS_2/C$ hybrid (inset) under the same condition: CV curves at various scan rates (**a**); GCD curves (**b**) and specific capacitances (**c**) at various current densities.

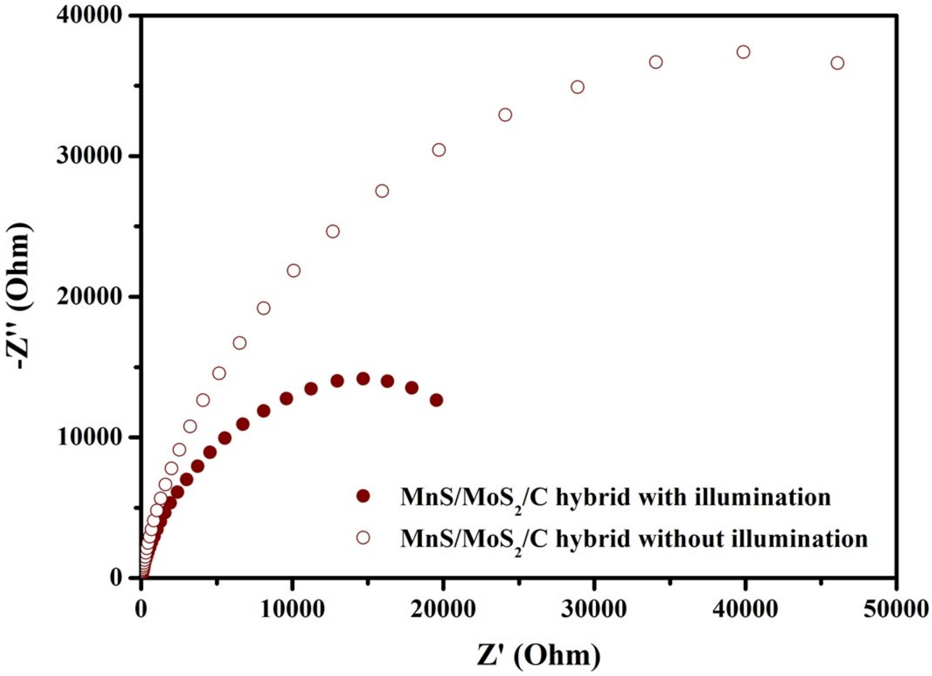

Fig. S21 The Nyquist plots (Z' vs $-Z''$) of the three-electrode systems at E = 0 V vs Hg/HgO in 2 M KOH solution in the absence and presence of visible light illumination (350 nm < λ < 650 nm) with the FTO working electrode of the $MnS/MoS_2/C$ hybrid.

(a)

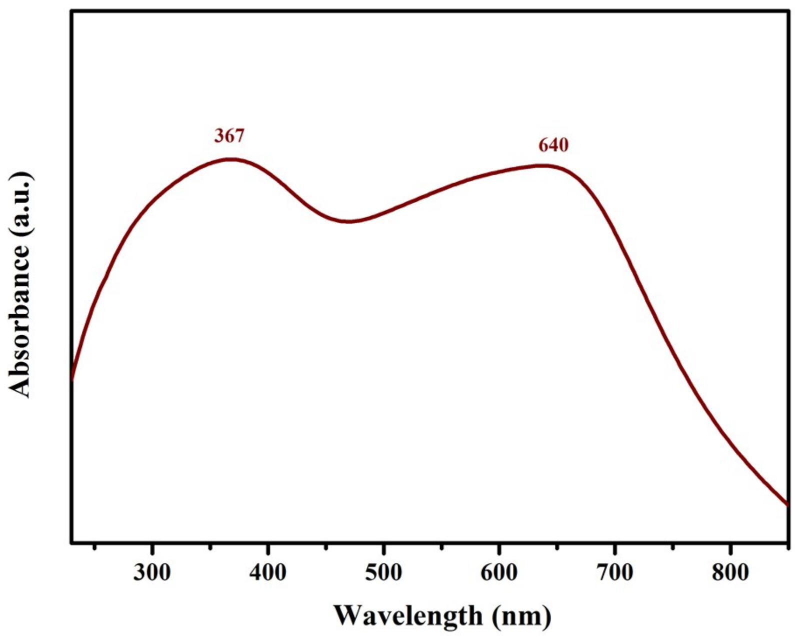

(**b**)

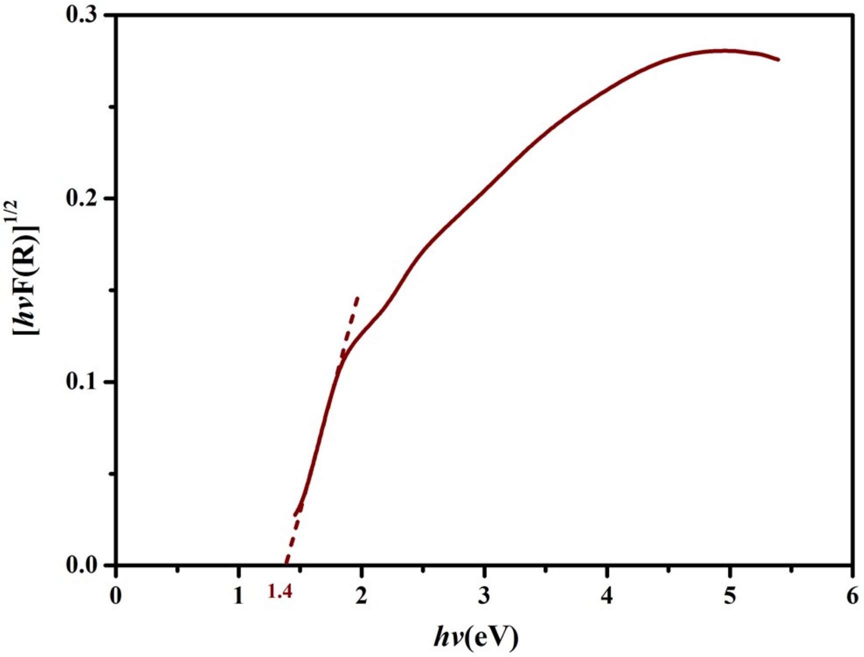

Fig. S22 The UV-vis absorption (**a**) and diffuse reflectance spectra of the $MnS/MoS_2/C$ hybrid in Kubelka-Munk functions (**b**).

The diffuse reflectance spectra of the $MnS/MoS_2/C$ hybrid are shown in **Fig. S20b**. The relationship between the absorption coefficient and band gap E_{gap} was determined by the equation:

$[h\nu F(R)]^{1/2} = A[h\nu - E_{gap}]$

Where $h\nu$ is the photon energy, A is a constant, F(R) is the Kubelka-Munk equation and $F(R) = (1-R)^2/2R$, in which R is the experimental value in reflectance of the sample.

According to the plot of $[h\nu F(R)]^{1/2}$ vs $h\nu$, the value of band gap E_{gap} of the sample can be obtained by extrapolating the linear fitted region to $[h\nu F(R)]^{1/2} = 0$.

(**a**)

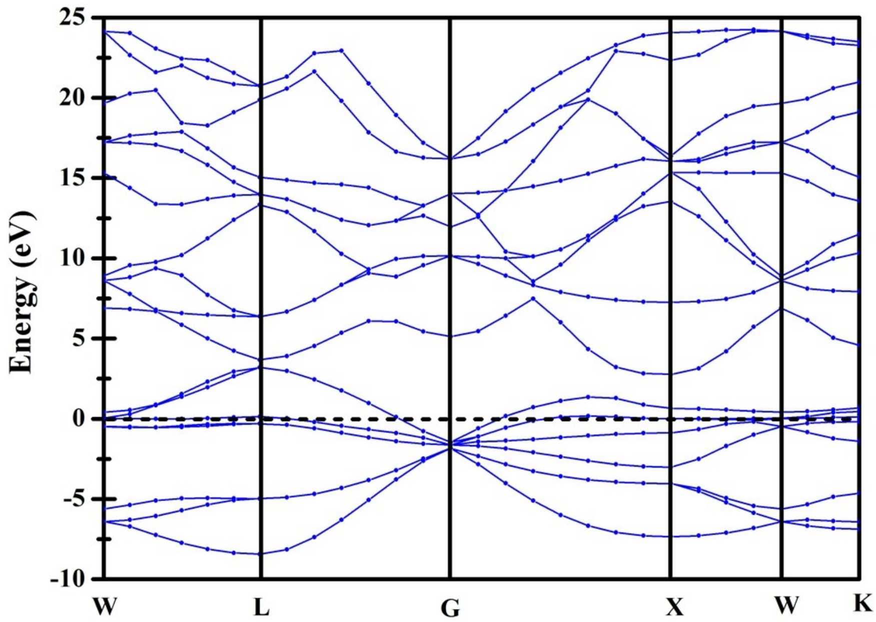

(**b**)

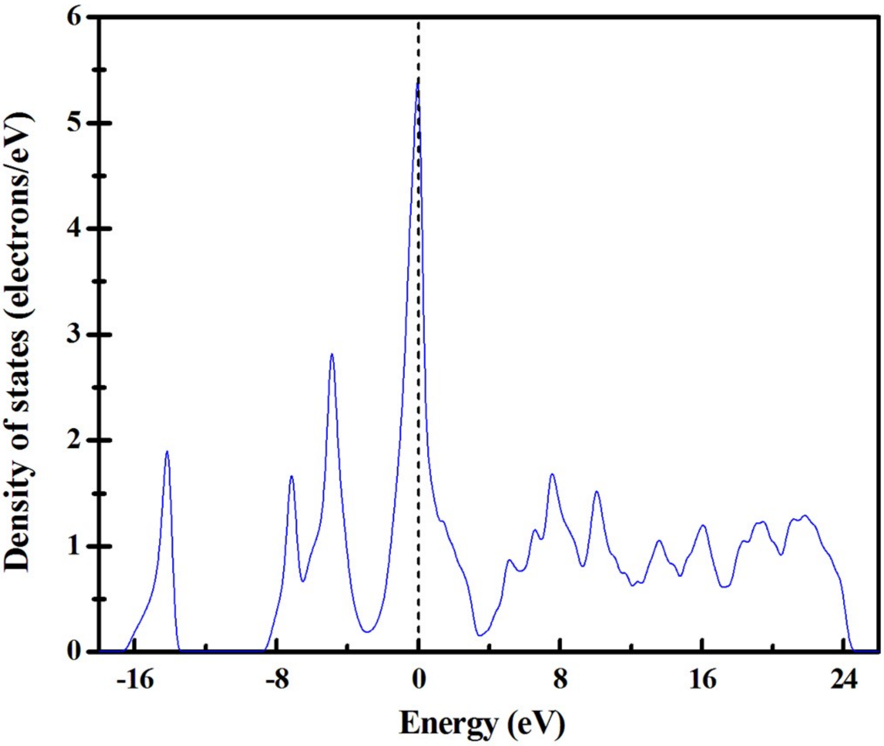

Fig. S23 Band structure (**a**) and the total density of states (TDOS) of the cubic MnS. (**b**). The Fermi level is set to zero

(**a**)

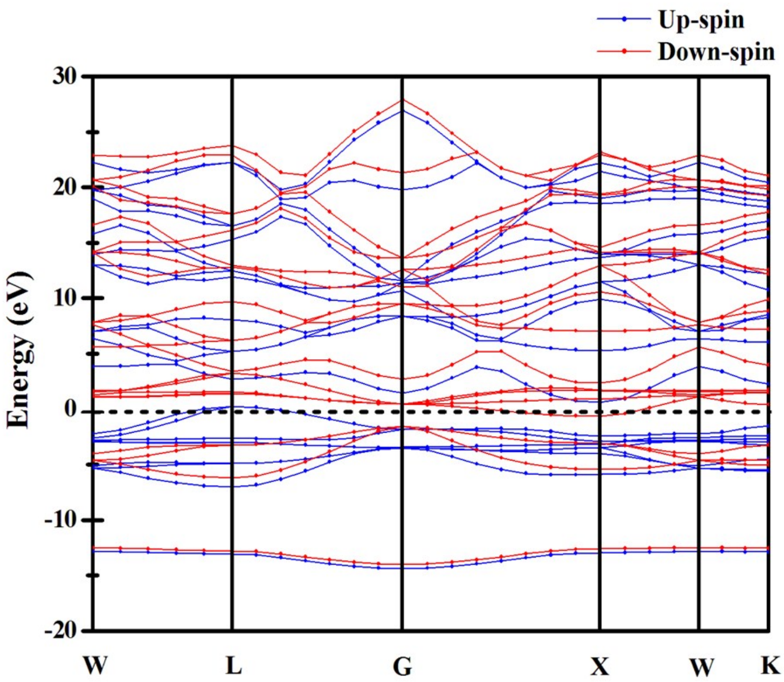

(**b**)

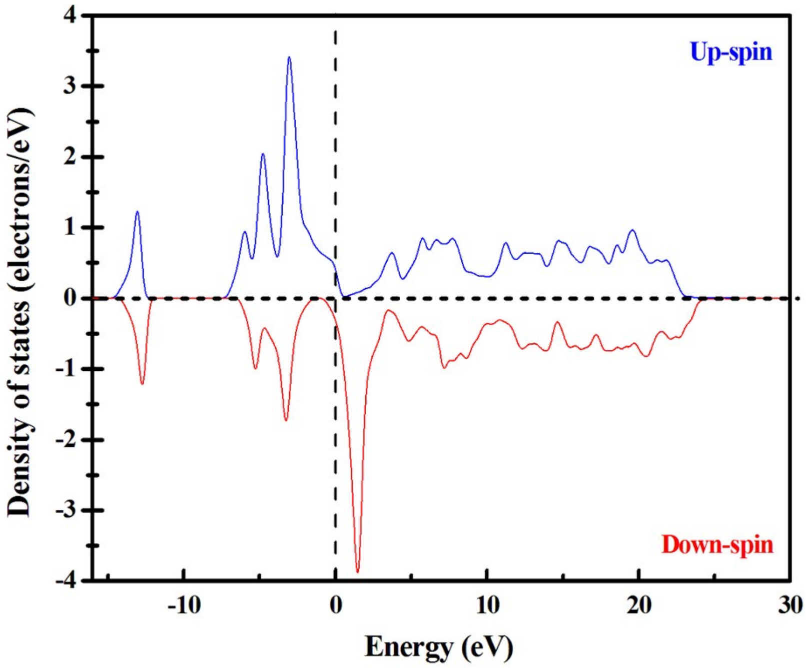

Fig. S24 Band structure (**a**) and TDOS of the spin-polarized cubic MnS (**b**). The blue and red curves correspond to the spin up and down bands, respectively. The Fermi level is set to zero.

(**a**)

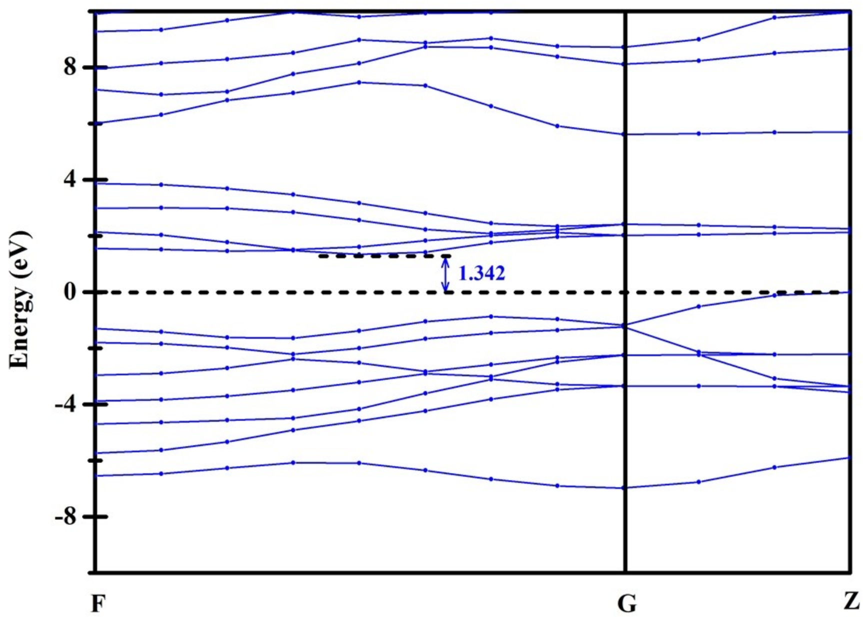

(**b**)

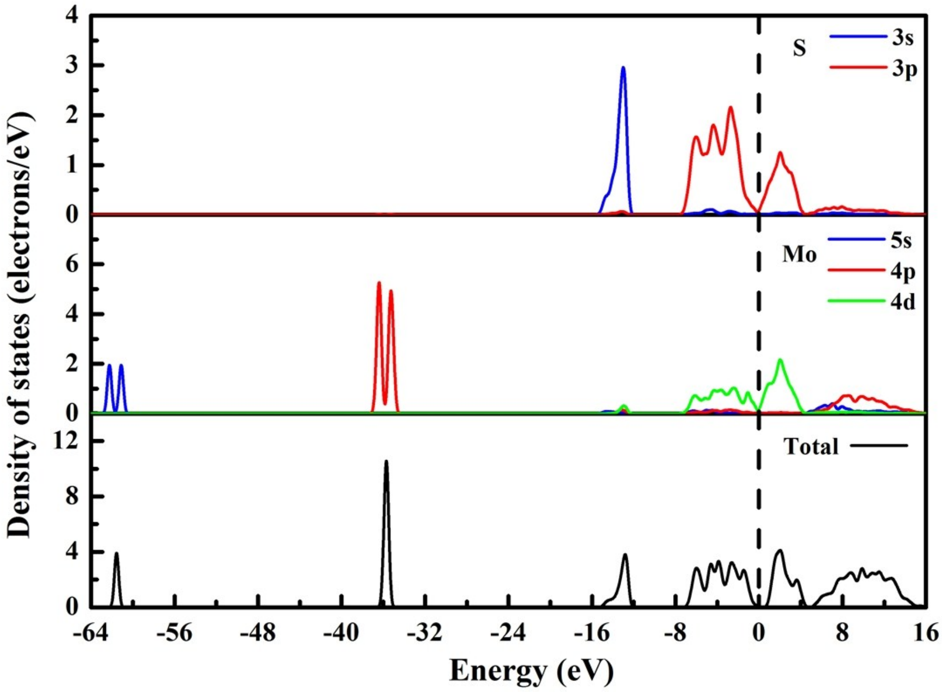

Fig. S25 Band structure (**a**) and TDOS as well as PDOS of the hexagonal MoS_2. In the PDOS, blue, red and green lines represent s, p and d orbits, respectively (**b**). The Fermi level is set to zero.

Table S2 The electrochemical performance comparisons of MnS/MoS2/C hybrid with other Mn/Mo sulfides based materials.

No.	Electrode material	Electrochemical testing condition (Three-electrode configuration)	Electrolyte	Specific capacitance	Reference
1	2D-MnS nanosheets	GCD at 0.5 A g^{-1}	2.0 M KOH	344.5 F g^{-1}	1
2	TP-NR MnS	CV at 1mV s^{-1}	2.0 M KOH	704.5 F g^{-1}	2
3	MnS/GO	GCD at 0.25 A g^{-1}	2.0 M KOH	390.8 F g^{-1}	3

4	MnS microfibers	CV at 5mV s^{-1}	1.0 M KOH	538.5 F g^{-1}	4
5	γ-MnS/rGO composite	GCD at 5 A g^{-1}	polysulfide electrolyte	802.5 F g^{-1}	5
6	Bulk MoS_2	GCD at 0.5 A g^{-1}	Organolithium intercalators	2.5 F g^{-1}	6
7	MoS_2 nanosheets	GCD at 0.5 A g^{-1}	1.0 M Na_2SO_4	92.8 F g^{-1}	7
8	MoS_2-carbon composite	GCD at 0.5 A g^{-1}	1.0 M Na_2SO_4	201.4 F g^{-1}	8
9	1T/2H Hybrid MoS_2	GCD at 1 A g^{-1}	2.0 M KOH	346.0 F g^{-1}	9
10	1T-2H MoS_2/rGO	GCD at 1 A g^{-1}	1.0 M NaCl	416.0 F g^{-1}	10
11	MoS_2 nanosheets with Co_3O_4	GCD at 0.5 A g^{-1}	1.0 M KOH	69.0 F g^{-1}	11
12	Ni_3S_4-MoS_2 heterojunction	GCD at 1 A g^{-1}	3.0 M KOH	985.2 F g^{-1}	12
13	MnS/MoS_2/C hybrid	GCD at 1 A g^{-1}	2.0 M KOH	1120 F g^{-1}	This work

References

1 M. Li, J. Liang, Y. Chai, D. L. Li, J. X. Lu and L. Li, *MICRO & NANO LETTERS*, 2017, **12**, 735-737.

2 Y. F. Tang, T. Chen and S. X. Yu, *Chem. Commun.*, 2015, **51**, 9018-9021.

3 Y. F. Tang, T. Chen, S.X. Yu, Y. Q. Qiao, S. C. Mu, J. Hua and F. M. Gao, *J. Mater. Chem. A*, 2015, **3**, 12913-12919.

4 R.B. Pujari, A.C. Lokhande, A.A. Yadav, J.H. Kim, C.D. Lokhande, *Materials and Design*, 2016, **108**, 510-517.

5 X. F. Li, J. F. Shen, N. Li and M. X. Ye, *J. Power Sources*, 2015, **282**, 194-201.

6 C. C. Mayorga-Martinez, A. Ambrosi, A. Y. S. Eng, Z. Sofer and M. Pumera, *Electrochem. Commun.*, 2015, **56**, 24-28.

7 K. Karthikeyan, V. Ganesh Kumar, R. Sivaprakasam and S. J. Kim, *Mater. Res. Bull.*, 2014, **50**, 499-502.

8 L. Fan, G. Liu, C. Zhang, J. Wu and Y. Wei, *Int. J. Hydrogen Energy*, 2015, **40**, 10150-10157.

9 D. Z. Wang, Y. Y. Xiao, X. N. Luo, Z. Z. Wu, Y. J.Wang and Baizeng Fang, *ACS Sustainable Chem. Eng.* 2017, **5**, 2509-2515.

10 A. Gigot, M. Fontana, M. Serrapede, M. Castellino, S. Bianco, M. Armandi, B. Bonelli, C. F. Pirri, E. Tresso and P. Rivolo, *ACS Appl. Mater. Interfaces* 2016, **8**, 32842-32852.

11 D. Lianga, Z. Tiana, J. Liu, Y. Ye, S. Wu, Y. Cai and C. Liang, *Electrochim. Acta*, 2015, **182**, 376-382.
12 W. H Luo, G. F. Zhang, Y. X. Cui, Y. Sun, Q. Qin, J. Zhang and W. *J. Zheng, J. Mater. Chem. A*, 2017, **5**, 11278-11285.